Seasonal variability of coccolith fluxes in sediment traps of the Perdido and Coatzacoalcos regions in the Southern Gulf of Mexico

Felipe de Jesús García-Romero[1*], Juan Carlos Herguera García[1], Jörg Bollmann[2], José Rubén Lara Lara[1], Mara Yadira Cortés Martinez[3], Amaru Márquez-Artavia[4]

[1]Division of Oceanography, Center for Scientific Research and Higher Education of Ensenada (CICESE), Ensenada, 22860 Mexico

[2]Department of Earth Sciences, Earth Sciences Centre, University of Toronto, 22 Ursula Franklin Street, Toronto, Ontario, M5S 3B1, Canada

[3]Department of Earth Science, Autonomous University of Baja California Sur, 23080, Mexico

[4]Escuela de Ciencias Biológicas. Universidad Nacional de Costa Rica.

*Corresponding author

fgarcia@cicese.edu.mx (FGR)

Abstract

We present new results of the coccolith fluxes in the Perdido and Coatzacoalcos regions of the Gulf of Mexico and explore the environmental variables that may control them. Two sediment trap moorings located at a water depth of 1100 m collected settling particles from June 2016 to July 2017. Both regions showed similar seasonal distributions in total coccolith fluxes, with the highest recorded fluxes during winter, decreasing through spring, and moderate fluxes in summer and autumn. The Perdido sediment trap shows slightly higher annual average fluxes of $3.09 \times 10^9 \pm 0.89 \times 10^9$ coccoliths per $m^{-2}d^{-1}$, in comparison to the Coatzacoalcos trap of $1.88 \times 10^9 \pm 1.13 \times 10^9$ coccoliths $m^{-2}d^{-1}$. The Perdido trap collected 47 species of coccoliths, in comparison with the Coatzacoalcos trap with 56 species throughout the study period. The species composition was dominant in both regions by *Emiliania huxleyi, Gephyrocapsa oceanica,* and *Florisphaera profunda*, reaching more than 85 %. The Upper Photic Zone (UPZ) species association was dominant throughout the study period, showing higher fluxes during winter, associated with the seasonal deepening of the mixed layer depth. In addition to the controls by the mesoscale forcings by the anticyclonic eddy (Poseidon) in the Perdido region and the semi-permanent cyclonic eddy (Campeche Bay) in Coatzacoalcos. The interaction between these mesoscale eddies with the continental shelf results in the advection of nutrient-rich waters to the deep ocean thereby increasing the coccolith productivity and consequently export-fluxes. Our results of the coccolith fluxes and the processes that modulate them in the Southwest of Mexico help to understand the different controls on the calcareous nannoplankton export in oligotrophic regions close to the continental shelf.

Keywords: Coccolith fluxes, Gulf of Mexico, Sediment trap, Seasonal variability, Perdido and Coatzacoalcos region.

Introduction

Coccolithophores are marine primary producers covered by calcareous plates called coccoliths that live in the ocean's photic zone and play a crucial role in the marine ecosystems [1] and show a high abundance in stratified nutrient-poor surface waters in the ocean [2]. When coccolithophores die, their coccolith remains are transported to the ocean floor in fecal pellets or marine snow at the end of their life cycle or when grazed by zooplankton [3, 4]. The analysis of coccoliths in sediment trap time-series provides significant information to understand the seasonal to inter-annual variability of the coccolithophores export flux to the deep ocean [5-10]. However, information about of variability of fluxes is still limited in the Gulf of Mexico.

Sediment-trap studies in the North Atlantic show strong seasonal patterns with maximum coccolith fluxes during spring bloom periods dominated by *Emiliania huxleyi* [7] and fast transport of coccoliths via fecal pellets in short pulses [6]. At the Bermuda station, the highest fluxes were recorded in late winter and spring. The coccolith assemblage was dominated by *E. huxleyi* and *Florisphaera profunda* and varied much less compared to the seasonal variability of the plankton assemblage in the photic zone and is potentially caused by patchiness plankton distribution, differential grazing, and the seasonally changing standing stock of coccolithophores [8]. In contrast, in the tropical North Atlantic, maximum fluxes occurred during summer and autumn and minimum in spring, and coccolithophore assemblages were dominated by the LPZ species (*F. profunda* and *Gladiolithus flabellatus*). High fluxes were associated with stronger stratification under the influence of the Intertropical Convergence Zone, and low fluxes occurred during stronger North Eastern trade winds and lowest sea surface temperatures during winter and spring [11].

In the Gulf of Mexico (GoM), most studies on coccolithophores have focused on the upper water column in the northern part of the GoM and show that coccolithophores are mainly affected by temperature, nutrient concentrations, light availability, and mixed layer depth, as well as mesoscale phenomena such as warm core eddies [12-18]. However, there is currently little known about the coccolith export flux and the seasonal to interannual variability of coccolithophore flux in this region, a prerequisite to understanding the environmental processes affecting coccolithophore production and their role in the global carbon cycle.

Here, we present data on coccolith fluxes and their seasonal variability from two sediment traps located in the Perdido and Coatzacoalcos regions, western and southwestern part of the GoM, and explore environmental parameters that might affect their production and flux.

Oceanographic conditions in the Gulf of Mexico

In the Gulf of Mexico (18°N to 30°N and 80°W to 98°W) (Fig 1) the circulation is mainly controlled by the Loop Current with sporadic spin-off of mesoscale anticyclonic eddies that move westward at a speed of 2 km d^{-1} [19-21]; these transient events can last up to a year [22, 23]. In the Bay of Campeche (southern region of GoM), a semi-permanent cyclonic eddy is present [24] that promotes Ekman pumping at its center resulting in the shallowing of the nutricline associated with the advection of nutrients into the euphotic zone [25]. Based on chlorophyll concentrations derived from satellite observation (Ocean color), the GoM basin can be divided into eutrophic coastal waters and oligotrophic “open ocean” deep waters of the central part of the GoM (roughly delimited by the 200 m isobath,) indicating low primary productivity in the open ocean and high primary productivity in coastal areas [26-28]. This is a result of low nutrient concentrations in the surface offshore waters spatially separated from eutrophic coastal waters [29, 30].

Fig 1. Study area in the southern Gulf of Mexico (GoM). Locations of sediment traps: the white triangles show the Perdido (P) in the North and Coatzacoalcos (C) in the South, and the black circles show the catchment area of the sediment trap from the environmental data extracted and processed. The color gradient indicates the bathymetric on the GoM. The dashed black line shows the 200 m isobath. White arrows show the direction of the loop current and the mesoscale structure: anticyclonic eddy at the North and semipermanent cyclonic eddy in the South in Campeche Bay.

Coupled physical-biogeochemical models and *in situ* bio-optical data show a seasonal variability of chlorophyll concentrations related to the injection of nutrients into the euphotic zone controlled by the deepening of the winter

mixed layer (ML) dynamic. In contrast, strong stratification during spring-summer is characterized by low nutrients and chlorophyll concentrations in the photic zone [28, 30, 31]. The deepening of the ML in winter is associated with mixing subsurface waters due to wind stress [32]. Furthermore, continental water discharges from sixteen rivers and wind stress also affect the nutrient availability especially on the shelves [33]. On the northern continental shelves of the GoM, the Mississippi and the Atchafalaya rivers in Louisiana and Texas significantly impact the ecosystem, with maximum water discharges in spring reaching 2.8 x 10^4 m^3 s^{-1}. In the southern region, the Grijalva-Usumacinta River complex and the Coatzacoalcos-Papaloapan rivers are major fresh water sources with maximum discharges in summer through early autumn with an annual flux of 0.38 x 10^4 m^3 s^{-1}. These river inputs supply nutrients and terrigenous sediments to the southern part of the Campeche Bay impact the phytoplankton growth dynamics in this region [29, 34, 35].

Oceanographic and meteorological conditions at Perdido and Coatzacoalcos during the study period

The Sea Surface Temperature (SST) decreases between late autumn and winter and increases in both regions from late spring to summer. SST shows higher amplitude in variability in the Perdido region (23.5-30.4°C) than in the Coatzacoalcos region (25.3-29.9°C). The Sea surface chlorophyll a (Chl-a) in the Perdido region shows low values in late spring to summer (0.079 mg m^3) and higher values in late autumn through winter (0.52 mg m^3). Similarly, the Coatzacoalcos region shows maximum values during late summer and early autumn (0.60 mg m^3) and low values in spring (0.15 mg m^3) (Fig 2 A). The mixed layer depth (MLD) was consistently deeper during late autumn until winter in both regions and shallower from spring to summer. The MLD in the Perdido region ranged between 10.5 to 68.3 m, whereas the Coatzacoalcos range was lower, between 7.2 m to 33.3 m. Wind speeds show a strong seasonality, with strong winds during autumn-winter and weaker winds in spring-summer. The Perdido region fluctuated between 3.9 and 7.0 m s^{-1}, while Coatzacoalcos fluctuated between 3.2 to 5.9 m s^{-1} (Fig 2 B). The summer to mid-autumn precipitation means were slightly higher in the Coatzacoalcos region (max 10.9 mm d^{-1}) than in the Perdido region (max 9.5 mm d^{-1}). In addition, the southern GoM was affected by the passage of tropical storm Danielle (June 19 to June 21) and category 1 hurricane Earl (2 to August 06)

(https://www.nhc.noaa.gov/data/tcr/index.php?season=2016&basin=atl). The passage of mesoscale eddies, observed in sea level anomaly (SLA) variability in the area, was further reflected in the recorded fluxes in the sediment trap. For the Perdido region, the core of the anticyclonic eddy was observed in mid-autumn, and the edge of the eddy was observed in winter. While in the Coatzacoalcos region, the core of a cyclonic eddy was observed during the summer and the edge in early autumn, the SLA presented a high fluctuation during the rest of the period from 0.12 to 0.08 m in spring (Fig 2 C).

Fig 2. Time series environmental variables to the Perdido and Coatzacoalcos traps. Datasets were downloaded from the catchment area for the Perdido and Coatzacoalcos traps (1° radius around sediment trap) throughout the study period. Sea Surface Temperature (magenta line) and Chlorophyll a (green line) variability A). Mixed Layer Depth (dark blue line) and wind speed (broken dark blue line) B). Precipitation (blue background), tropical storm Danielle, and hurricane Earl (category 1), which affected the Coatzacoalcos region to a greater extent, are highlighted. Sea Level Anomaly (Orange line): High values show an anticyclonic eddy core and low values show the anticyclonic eddy border for the Perdido trap. Low values denote a cyclonic eddy and high values show a cyclonic eddy bordering the Coatzacoalcos trap C). Light and dark grey bands refer to the season of the year.

Material and methods

Trap deployment and sample treatment

Two sediment traps were deployed in the western and southwest Gulf of Mexico, in the Perdido and Coatzacoalcos region, at 1100 m and 1050 m water depth (55 m above the sea floor each one) respectively, collecting sinking particles from June 2016 to July 2017. Each cup was open for 18 days (Fig 1, Table 1). Each

mooring was equipped with a McLane automated time-series sediment trap, model Par flux Mark 78H-21 with a 0.5 m^{-2} collection opening cone, and twenty-one collection bottles of 500 ml capacity. Each collection bottle was prefilled with a preserving 4% formaldehyde water solution to minimize biological decomposition, filtered (0.45 µm) seawater, buffered with sodium tetraborate, and sodium chloride (both high purity) to 8.5 pH to minimize the dissolution of carbonates [36].

Trap samples were sieved through a 1000 µm Nylon screen to remove "swimmers" [37, 38]. After sieving, each sample was divided into ten equal subsamples (50 ml each) using a wet sampler divider (WSD-10 McLane Laboratory) with deviations between aliquots <5.0% [39].

Table 1. Sediment trap mooring information deployed in the Gulf of Mexico. There is a deface in the first sample of the Perdido trap because it was not possible to install the sediment trap due to the passage of Tropical Storm Danielle (Jun 19 to Jun 21). In both traps, the events total 378 sampling days. Sample lost during sediment trap recovery (*).

Location	Perdido trap		Coatzacoalcos trap		
	25.43111° N and 96.07207° W		19.3867° N and 94.0597° W		
Event no.	Begin date	End date	Event no.	Begin date	End date
			1	6/16/2016	7/3/2016
1*	7/4/2016	7/21/2016	2	7/4/2016	7/21/2016
2	7/22/2016	8/8/2016	3	7/22/2016	8/8/2016
3	8/9/2016	8/26/2016	4	8/9/2016	8/26/2016
4	8/27/2016	9/13/2016	5	8/27/2016	9/13/2016
5	9/14/2016	10/1/2016	6	9/14/2016	10/1/2016
6	10/2/2016	10/19/2016	7	10/2/2016	10/19/2016
7	10/20/2016	11/6/2016	8	10/20/2016	11/6/2016
8	11/7/2016	11/24/2016	9	11/7/2016	11/24/2016
9	11/25/2016	12/12/2016	10	11/25/2016	12/12/2016
10	12/13/2016	12/30/2016	11	12/13/2016	12/30/2016
11	12/31/2016	1/17/2017	12	12/31/2016	1/17/2017
12	1/18/2017	2/4/2017	13	1/18/2017	2/4/2017
13	2/5/2017	2/22/2017	14	2/5/2017	2/22/2017
14	2/23/2017	3/12/2017	15	2/23/2017	3/12/2017
15	3/13/2017	3/30/2017	16	3/13/2017	3/30/2017
16	3/31/2017	4/17/2017	17	3/31/2017	4/17/2017
17	4/18/2017	5/5/2017	18	4/18/2017	5/5/2017
18	5/6/2017	5/23/2017	19	5/6/2017	5/23/2017
19	5/24/2017	6/10/2017	20	5/24/2017	6/10/2017
20	6/11/2017	6/28/2017	21	6/11/2017	6/28/2017
21	6/29/2017	7/16/2017			

Coccolith analysis

The pre-split samples were further wet split into smaller aliquots employing a Sampler Rotatory Divider Laborette 27, (split of 2/60). We calculated the standard error by analyzing four samples in triplicate (3, 10, 14, and 21 for each sample set), resulting in a 0.4 % error between splits. After fecal pellets were disintegrated and the organic matter was removed [40], samples were filtered onto Nucleopore membranes (47 mm diameter, 0.45 µm pore size). A piece of the membrane filter was mounted on aluminum stubs and sputtered with 3 nm of platinum using a BalTec SCD500 sputter for subsequent automated acquisition of 500 images per sample at 1500 X

magnification on a scanning electron microscope (Zeiss Supra 55VP) [41]. The total area covered by the 500 images is 2.13 x 10^{-6} m^{-2} per sample.

The image analysis software *Image-J for Windows*® was used to count (custom plugin) and measure the size of coccoliths. Additionally, coccolith fragments (ranging from 25 to 75% visual inspection) were quantified and used to calculate the number of coccoliths. The coccolith flux (coccoliths m^{-2} d^{-1}) was calculated following Andruleit (42).

Eq. (1):

$$Cf = \frac{N * A * Sf}{a * t * Mt}, \quad (1)$$

where *Cf*= Coccolith flux; N = number of coccoliths; A = Effective filtered area (9.89E^{-04} m^{-2}); Sf= Split factor (4500); a = analysed filter area (2.13083E^{-06} m^{-2}); t = sediment collection time (18 days), and Mt = Mouth of sediment trap (0.5 m^{-2}).

The relative abundance for each coccolith species in each sample was calculated as the following equation:

$$\boldsymbol{RA = \frac{ni}{N} * 100} \quad \textbf{(2)}$$

Where *RA*= Relative abundance (%), *ni*= number of coccoliths of specie *i*, and *N*= Total number of coccoliths in the sample.

The general identification of coccoliths includes the identification of morphotypes of *Emiliania huxleyi* type A (*huxleyi*), type B (*pujosiae*), and *E. huxleyi* var. *corona*. followed the taxonomic concept described by Young, Geisen (43) and the Nannotax web site (https://www.mikrotax.org/Nannotax3/index.html Accessed 21 Apr. 2022). Morphotypes of *Florisphaera profunda* were identified according to Quinn, Cortes (44), morphotypes of *Gephyrocapsa oceanica, G. muellerae, and G. ericsonii* were identified according to Bollmann (45), and species within *Syracosphaera* group were identified according to Kleijne and Cros (46). All coccoliths were identified to

species level except for some specimens of *Syracosphaera*, which are reported as spp. Taxa with an average relative abundance larger than 2 % are referred to as “most common taxa”, while species with relative abundances less than 2 % are referred to as “Other coccoliths” in the entire manuscript.

Ecological indices

We used the number of species observed in the sample as the species richness "S", for the diversity index we used Shannon and Weaver (47); calculated with the following equation:

$$H' = -\sum_{i=1}^{s} Pi * lnPi \quad \textbf{(3)}$$

Where: H´=diversity; S = the number of species; P*i* = relative or proportional abundance of *i* species (equal to ni/N), where ni is the number of coccoliths by species and N is the total number of coccoliths. For the Evenness we used Pielou (48) with the following equation:

$$J = \frac{H'}{\ln(s)} \quad \textbf{(4)}$$

Where: H’ is Shannon Weaver's diversity and (s) the number of species observed in the sample. Finally, the dominance index Berger and Parker (49) "d" with the following equation:

$$d = \frac{nmax}{N} \quad \textbf{(5)}$$

Where: *d* = dominance index; *nmax* = the number of individuals of the most abundant species, and *N* = the total number of individuals in the sample.

We grouped the coccolithophore assemblages into the upper photic zone (UPZ) and lower photic zone (LPZ) based on their reported ecological preferences from plankton studies [2, 50-53]. The ratio between the UPZ/LPZ taxa was used to identify variations of the nutricline [52, 54] since the boundary between LPZ and UPZ is approximately the position of the deep chlorophyll maximum, nutricline, and PAR at a level of 1% [55].

Remote sensing data

Surface oceanographic data from remote sensing and numerical models were retrieved within a one-degree radius around each sediment trap location. This area potentially includes the source regions of sinking aggregates and marine phytoplankton reaching the sediment trap at 1100 m water depth (e.g. [56]). Surface data were additionally averaged over the 18-day collecting period of each sediment trap cup to relate the oceanographic surface variability with the sediment trap data. The surface time series were also used on the ordination of the multivariate analysis described in the next section. Data sources and more detailed information are given in the supplementary material (S1).

Sea Surface Temperature (SST) was used as a proxy for thermal stratification [57]. Sea surface chlorophyll a (Chl-a) was used as an indicator of primary productivity variability [58]. To determine the presence of cyclonic and anticyclonic eddies within the radius of influence of sediment traps, we used sea level anomaly (SLA) data from the Copernicus Marine Service (CMEMS; https://doi.org/10.48670/moi-00148). Wind Speed (WS) data [59, 60] allow us to identify the occurrence of strong wind bursts known as the "Nortes" related to outbreaks of cold air from North America during late autumn and winter. These winds provide mechanical energy and heat fluxes to the sea surface and control the Mixed layer Depth (MLD) [61] and consequently, nutrient availability and Photosynthetic Available Radiation (PAR) [62]. Precipitation (PREC) can provide information for the general understanding of weather patterns and seasonality [63] and, indirectly, the freshwater influx from rivers into the Perdido and Coatzacoalcos region.

Statistical analysis

Principal Components Analysis (PCA) was performed with a correlation matrix that included environmental parameters and the most abundant taxa as well as the “Other coccoliths” group. The relationship between the flux of coccoliths and environmental parameters during the study period was explored with the aid of a Spearman rank correlation and Canonical Correspondence Analysis. These analyses provide an integrated description of the species-environment relationship allowing for the identification of the environmental factors that best explain

the variation in the assemblage composition [64]. We used the software package Past 4.03. The data matrix included Mixed Layer Deep (MLD), Sea Level Anomaly (SLA), Geostrophic Speed (GOS), Wind Speed (WS), Precipitation, Photosynthetically Active Radiation (PAR), Sea Surface Temperature (SST), Sea Surface Salinity (SSS), Chlorophyll a (CHL) and the Coccolith fluxes.

Results:

In total, forty-one samples were recovered: twenty for Perdido (sample 1 was lost: 07/04/2016-07/21/2016) and twenty-one for Coatzacoalcos. Sixty-eight taxa were identified in this study (Table 2).

Table 2. **Taxonomic list of coccolithophore species recorded for the Perdido and Coatzacoalcos traps.** The scientific name of the taxa, Current citation, and location: Perdido = P and Coatzacoalcos = C, as well as coccolith type: Heterococcolith = HET, Holococcolith = HOL, Nannolith = NAN. The dinoflagellate = DIN was recorded.

TAXA	Current citation
Acanthoica acanthifera	Lohmann 1912 ex Lohmann, 1913
Acanthoica acanthos	Schiller 1925
Acanthoica quattrospina	Lohmann 1903
Acanthoica sp.	Lohmann 1903
Algirosphaera robusta	(Lohmann 1902) Norris, 1984
Braarudosphaera bigelowi	(Gran & Braarud 1935) Deflandre, 1947
Calcidiscus leptoporus small	(Murray & Blackman 1898) Loeblich & Tappan, 1978
Calciosolenia brasiliensis	(Lohmann, 1919) Young in Young *et al*., 2003
Calciosolenia murrayi	Gran, 1912
Calyptrosphaera oblonga	Lohmann 1902
Ceratolithus cristatus	Kamptner 1950
Ceratolitus cristatus	(Kamptner 1950) CER cristatus type sensu Young *et al*., 2003
Coccolithus pelagicus	(Wallich 1877) Schiller, 1930
Coronosphaera mediterranea	(Lohmann 1902) Gaarder, in Gaarder & Heimdal, 1977 [according to Triantaphyllou *et al*. 2016 and Young *et a*
Cyrtosphaera aculeata	(Kamptner 1941) Kleijne, 1992
Cyrtosphaera cidaris	(Schlauder 1945) Young & Bown 2014
Discosphaera tubifera	(Murray & Blackman 1898) Ostenfeld, 1900
Emiliania huxleyi type A	(Lohmann 1902) Hay & Mohler, in Hay *et al*. 1967
Emiliania huxleyi type B	Young & Westbroek, 1991
Emiliania huxleyi var. *Corona*	(Okada & McIntyre 1977) Jordan & Young, 1990
F. profunda var. *Elongata*	Okada & MacInyre 1980
F.profunda var. *Rhinocera*	Quinn *et al*., 2005
Florisphaera profunda	Okada & Honjo, 1973
Gephyrocapsa ericsonii	(McIntyre & Bé, 1967)
Gephyrocapsa mullerae	Bréhéret, 1978
Gephyrocapsa oceanica	Kamptner, 1943
Gladiolithus flabellatus	(Halldal & Markali 1955) Jordan & Chamberlain, 1993
Hayaster perplexus	(Bramlette & Riedel 1954) Bukry, 1973
Helicosphaera carteri	(Wallich 1877) Kamptner, 1954
Helicosphaera pavimentum	Okada & McIntyre, 1977
Helicosphaera wallichii	(Lohmann 1902) Okada & McIntyre, 1977
Michaelsarsia elegans	Gran, 1912
Oolitothus antillarum	(Cohen 1964) Reinhardt, in Cohen & Reinhardt, 1968
Oolitothus fragilis	(Lohmann 1912) Martini & Müller, 1972
Ophiaster formosus	Gran, 1912
Ophiaster hydroideus	(Lohmann 1903) Lohmann, 1913
Ophiaster reductus	Manton & Oates, 1983
Palusphaera vandelli	Lecal, 1965
Papposphaera spp.	Tangen, 1972
Ponthosphaera spp.	Lohmann, 1902
Pontosphaera multipora	(Kamptner, 1948 ex Deflandre in Deflandre & Fert, 1954) Roth, 1970
Poricalyptra spp.	Kleijne 1991
Reticulofenestra parvula	(Okada & McIntyre 1977) Bendif, Probert, Young & von Dassow in Bendif *et al*. 2016
Reticulofenestra sessilis	(Lohmann 1912) Jordan & Young, 1990
Reticulofenestra sp.	Hay, Mohler & Wade, 1966
Rhabdosphaera clavigera var. *stilifera*	(Lohmann, 1902) Kleijne&Jordan, 1990
Scyphosphaera apsteinii	Lohmann, 1902
Solisphaera blagnasensis	Bollmann *et al*., 2006

Forty-seven coccolith species were recorded throughout the studied period in the Perdido trap; species richness ranged from 16 in early winter to 40 species in late autumn, the Shannon-Weaver diversity index ranges from 0.8 in late winter to 1.6 in mid-autumn, the evenness values range from 0.08 in late winter to 0.18 in early winter, and the Berger Parker dominance index ranges from 0.4 during late autumn to 0.8 in late winter. The Coatzacoalcos trap collected 56 species during the deployment period and showed a minimum of 8 species mid-spring and a maximum of 41 species in the early spring. The Shannon-Weaver diversity index ranges from 0.8 in late spring to 1.7 in mid-autumn, the evenness ranges from 0.08 in early spring to 0.5 in mid-spring, the dominance index ranges from 0.4 in early autumn to 0.7 in mid-winter and late spring (Fig 3 A).

Assemblage composition of coccolithophores

Out of all taxa recorded in the sediment traps, only seven showed a relative abundance >2 % on average in the study period “most common taxa”. *Emiliania huxleyi* type A was the dominant specie in the Perdido trap, averaging 61 %, and the most abundant in the Coatzacoalcos trap with 46 %. Other common species included *Gephyrocapsa oceanica,* averaging 10 % in Perdido and 13 % in the Coatzacoalcos. *Florisphaera profunda* var. *elongata* (small) averaged 8 % in Perdido and 10 % in Coatzacoalcos. *F. profunda* var. *profunda* (small) recorded 5 % in Perdido and 13 % in Coatzacoalcos. *Umbellosphaera tenuis* averaged 2% in Perdido and 2 % in Coatzacoalcos. *Gladiolithus flabellatus* averaged 2 % in both regions. *F. profunda* var. *elongata* (medium) averaged 3 % in Perdido and 1 % in Coatzacoalcos. *E. huxleyi* type B averaged 2 % in Perdido and 2 % in Coatzacoalcos. The group “Other coccoliths” in the Perdido trap reached 8 % and 10 % in the Coatzacoalcos trap (Fig 3 B, Table 3).

Fig 3. Ecological index to the Perdido and Coatzacoalcos traps. Species richness (blue bars), Shannon-Weaver diversity (green line with dots), Evenness (black dotted line), and Berger-Parker dominance index (purple color). The y-axis on the left shows the number of species, while the y-axis on the right shows the Shannon-

Weaver, Evenness, and Dominance A). The relative abundance (%) of the taxa for each sample. Taxa with lower relative abundances (<2%) are grouped in "Other coccoliths" B).

Table 3. Relative abundances and coccolith fluxes (x 10^9) for the Perdido and Coatzacoalcos traps. Range, average, and standard deviation for each case. Relative abundance > 2 % on average throughout the study period was considered abundant coccolithophore taxa (loadings marked and *), while relative abundances < 2 % were grouped in Other coccoliths. Relative abundances < 0.05 on average are shown to three decimal places.

Taxa	Relative abundances (%)			
	Min	Max	Average	StDev
Total flux coccoliths				
***E. huxleyi* type A ***	40.9	77.2	61.3	10.0
***G. oceanica** *	3.3	23.2	10.2	6.7
***F. profunda* var. *elongata* small ***	1.6	14.3	8.1	3.7
***F. profunda* var. *profunda* small ***	0.8	11.6	5.4	2.6
***F. profunda* var. *elongata* medium ***	0.4	6.0	2.7	1.6
***U. tenuis** *	0.4	5.1	2.3	1.3
***G. flabellatus** *	0.2	4.5	2.1	1.6
Others coccoliths	3.4	14.2	7.8	2.7
E. huxleyi type B	0.2	4.3	1.9	1.0
U. irregularis	0.3	3.9	1.5	0.9
U. sibogae	0.3	2.1	0.9	0.5
S. pulchra	0.0	1.3	0.7	0.4
F. profunda var. *elongata* large	0.1	0.9	0.4	0.3
H. carteri	0.0	0.5	0.3	0.1
F. profunda var. *profunda* medium	0.0	0.5	0.3	0.1
C. leptoporus	0.1	0.5	0.2	0.1
C. brasiliensis	0.0	1.0	0.2	0.3
C. cristatus HET	0.0	0.4	0.2	0.1
U. hulburtiana	0.0	0.3	0.1	0.1
G. ericsonii	0.0	0.3	0.1	0.1
R. sessilis	0.0	0.3	0.1	0.1
G. mullerae	0.0	0.3	0.1	0.1
U. foliosa	0.0	0.5	0.1	0.1
F. profunda var. *rhinocera*	0.0	0.3	0.1	0.1
Reticulofenestra sp.	0.0	0.5	0.1	0.1
S. molischii	0.0	0.3	0.1	0.1
S. lamina	0.0	0.4	0.1	0.1
R. clavigera	0.000	0.403	0.060	0.122
C. murrayi	0.000	0.213	0.048	0.064
H. perplexus	0.000	0.161	0.040	0.051
H. wallichii	0.000	0.128	0.040	0.039
S. nana	0.000	0.202	0.039	0.058
D. tubifera	0.000	0.370	0.029	0.084
C. pequeña	0.000	0.107	0.029	0.030
C. Cristatus CER	0.000	0.157	0.028	0.037
R. clavigera var. *stylifera*	0.000	0.149	0.018	0.039
O. antillarum	0.000	0.059	0.016	0.016
M. elegans	0.000	0.072	0.015	0.024
O. formosus	0.000	0.236	0.014	0.053
S. apsteinii	0.000	0.098	0.014	0.025

Taxa	Relative abundances (%)			
	Min	Max	Average	StDev
Total flux coccoliths				
***E. huxleyi* type A ***	6.5	71.5	46.1	19.9
***F. profunda* var. *profunda* small ***	0.6	52.7	13.5	15.8
***G. oceanica ***	3.3	43.5	13.3	11.3
***F. profunda* var. *elongata* small ***	0.8	30.0	10.0	8.8
***E. huxleyi* type B ***	0.0	8.7	2.4	2.2
***U. tenuis ***	0.4	8.5	2.4	1.8
***G. flabellatus ***	0.0	9.3	2.1	2.0
Others coccoliths	4.5	17.9	10.2	4.1
U. sibogae	0.0	3.9	1.5	1.2
F. profunda var. *elongata* medium	0.0	5.2	1.3	1.3
U. irregularis	0.0	3.1	1.1	0.9
S. pulchra	0.0	2.7	0.9	0.8
C. cristatus HET	0.0	7.2	0.8	1.7
H. carteri	0.0	1.1	0.5	0.3
C. brasiliensis	0.0	1.7	0.5	0.5
F. profunda var. *profunda* medium	0.0	1.4	0.4	0.4
C. leptoporus small	0.0	3.4	0.3	0.7
Discosphaera tubifera	0.0	1.6	0.3	0.4
F. profunda var. *elongata* large	0.0	1.5	0.3	0.3
R. clavigera var. *clavigera*	0.0	0.7	0.2	0.3
C. leptoporus	0.0	0.8	0.2	0.2
S. tumularis	0.0	1.7	0.2	0.4
R. sessilis	0.0	0.6	0.2	0.2
O. antillarum	0.0	1.7	0.2	0.4
S. nana	0.0	0.9	0.1	0.2
F. profunda var. *rhinocera*	0.0	0.6	0.1	0.1
R. clavigera var. *stylifera*	0.0	0.4	0.1	0.1
U. hulburtiana	0.0	0.3	0.1	0.1
Poricalyptra sp.	0.0	0.4	0.1	0.1
S. molischii	0.0000	0.1952	0.0594	0.0645
C. cristatus CER	0.0000	0.4082	0.0563	0.0919
G. ericsonii	0.0000	0.3287	0.0552	0.0741
H. perplexus	0.0000	0.2874	0.0551	0.0702
O. formosus	0.0000	0.4326	0.0521	0.1267
C. cidaris	0.0000	0.4790	0.0519	0.1250
C. murrayi	0.0000	0.2762	0.0483	0.0729
G. mullerae	0.0000	0.2105	0.0473	0.0609
C. pelagicus	0.0000	0.4082	0.0455	0.0897
H. wallichii	0.0000	0.2020	0.0442	0.0497
C. mediterranea	0.0000	0.2778	0.0421	0.0700

Total coccolith flux

Coccolith fluxes consistently showed a seasonal pattern with high fluxes in winter (December 21 – March 21) and low fluxes in spring (March 19 – June 20) (Fig 4 A) at both locations. The annual average coccolith fluxes in the Perdido trap are 62% higher than the flux in the Coatzacoalcos trap with an annual average flux of 3.09 x 10^9± 0.89 x 10^9 coccoliths per $m^{-2}d^{-1}$ and 1.88 x 10^9 ± 1.13 x 10^9 coccoliths $m^{-2}d^{-1}$, respectively. The Perdido trap shows high fluxes in summer (June 20 – September 22) and autumn (September 22 – December 21) and a rapid decline during late autumn and early winter, resulting in the lowest flux observed during the entire period (1.30 x 10^9 coccoliths per $m^{-2}d^{-1}$). Fluxes increase again towards mid-winter with a maximum of 4.29 x 10^9 coccoliths per $m^{-2}d^{-1}$ after decreasing towards spring. The flux in the Coatzacoalcos trap ranged from 1.01 x 10^9 coccoliths per $m^{-2}d^{-1}$ to 3.10 x 10^9 coccoliths per $m^{-2}d^{-1}$ in summer and autumn, with the highest flux of 3.78 x 10 10^9 coccoliths per $m^{-2}d^{-1}$ in mid-winter, in early spring shows a peak of 2.61 x 10^9 coccoliths per $m^{-2}d^{-1}$, subsequently the values decrease drastically reaching a minimum of 0.013 x 10^9 coccoliths per $m^{-2}d^{-1}$. The normalized fluxes showed a general trend where, in both regions, the values decreased towards the spring and summer of 2017 (Fig 4 B).

Fig 4. Seasonality of total coccolith fluxes and Normalized fluxes. Total coccolith fluxes units in coccoliths per m^{-2} d^{-1} x 10^9 (blue bars) A) and the normalized flux, deviation from the annual mean coccolith flux with the sample number for the Perdido and Coatzacoalcos traps B).

Flux of individual species

The main contributor to the total coccolith fluxes in both regions was *E. huxleyi type* A, which in the Perdido trap recorded a higher flux of 3.3 x 10^9 coccoliths per $m^{-2}d^{-1}$ in late winter-early spring. In contrast, in the Coatzacoalcos trap, the maximum flux was 2.7 x 10^9 coccoliths per $m^{-2}d^{-1}$ in mid-winter (Fig 5 A). *G. oceanica*

reached a maximum flux of 0.8 x 10^9 coccoliths per $m^{-2}d^{-1}$ in the mid-winter in the Perdido trap and 1.3 x 10^9 coccoliths per $m^{-2}d^{-1}$ in late autumn in the Coatzacoalcos trap (Fig 5 B). *F. profunda* var. *elongata* (small) showed a higher flux of 0.41 x 10^9 coccoliths per $m^{-2}d^{-1}$ in early autumn in the Perdido trap; values decrease towards winter and increase again in spring. At the same time, the Coatzacoalcos trap recorded a maximum flux of 0.36 x 10^9 coccoliths per $m^{-2}d^{-1}$ in late spring of 2016 (Fig 5 C). *F. profunda* var. *profunda (small*) reaches a maximum flux of 0.29 x 10^9 coccoliths per $m^{-2}d^{-1}$ in late summer and early autumn in the Perdido trap and 0.44 x 10^9 coccoliths per $m^{-2}d^{-1}$ in late summer and early autumn in the Coatzacoalcos trap (Fig 5 D). The flux of *U. tenuis* was 0.51 x 10^9 coccoliths per $m^{-2}d^{-1}$ during late winter in the Perdido trap and 0.09 x 10^9 coccoliths per $m^{-2}d^{-1}$ in late summer in the Coatzacoalcos trap (Fig 5 E). *G. flabellatus* reached a maximum of 0.15 x 10^9 coccoliths per $m^{-2}d^{-1}$ in early spring in the Perdido trap and 0.16 x 10^9 coccoliths per $m^{-2}d^{-1}$ in early autumn in the Coatzacoalcos trap (Fig 5 F). *F. profunda* var. *elongata* (medium) showed the highest flux of 0.19 x 10^9 coccoliths per $m^{-2}d^{-1}$ in early autumn in the Perdido trap and of 0.43 x 10^9 coccoliths per $m^{-2}d^{-1}$ from late spring into early summer 2016 in the Coatzacoalcos trap (Fig 5 G). *E. huxleyi* type B reached a maximum flux of 0.13 x 10^9 coccoliths per $m^{-2}d^{-1}$ in mid-winter for the Perdido trap and 0.21 x 10^9 coccoliths per $m^{-2}d^{-1}$ in mid-autumn in the Coatzacoalcos trap (Fig 5 H). The group “Other coccoliths” in the Perdido trap reached a flux of 0.49 x 10^9 coccoliths per $m^{-2}d^{-1}$ in mid-autumn. The Coatzacoalcos trap showed a high flux of 0.43 x 10^9 coccoliths per $m^{-2}d^{-1}$ in the late summer (Fig 5 I). In this group, *U. irregularis* shows a maximum flux of 0.13 x 10^9 coccoliths per $m^{-2}d^{-1}$ to mid-autumn in the Perdido trap and 0.07 x 109 coccoliths per $m^{-2}d^{-1}$ to mid-summer in Coatzacoalcos (Fig J). *U. sibogae* showed a maximum flux of 0.07 x 10^9 coccoliths per $m^{-2}d^{-1}$ in the mid-summer of 2016 to the Perdido trap and 0.09 x 10^9 coccoliths per $m^{-2}d^{-1}$ during the mid-summer of 2016 for Coatzacoalcos trap (Fig 5 K). *S. pulchra* reached a maximum flux of 0.04 x 10^9 coccoliths per $m^{-2}d^{-1}$ during late autumn and 0.06 x 10^9 coccoliths per $m^{-2}d^{-1}$ during mid-autumn to the Coatzacoalcos trap (Fig 5 L).

Fig 5. Seasonality of individual species. Coccolith fluxes units coccoliths per m^{-2} d^{-1} x 10^9 (blue bars) and relative abundances (% orange lines) for the Perdido and Coatzacoalcos traps. Light and dark grey bands refer to the

season of the year. The taxa marked with bold letters presented relative abundances more significant than 2% throughout the study period; the rest of the coccoliths taxa with relative abundances <2 % were grouped in "Other coccoliths". Some of the significant contributors to this group were *U. irregularis, U. sibogae,* and *S. pulchra.* The composition of more abundant taxa is different for the Perdido trap than for Coatzacoalcos, but they have been sorted for comparative purposes only (see Table 3).

Seasonal variation of coccolith species associated with the upper and lower photic zone

The Upper Photic Zone (UPZ) coccolith assemblage includes the species: *E. huxleyi* type A and B, *G. oceanica*, *U. tenuis*, *U. irregularis*, and *U. sibogae* and the Lower Photic Zone (LPZ) assemblage includes *G. flabellatus* and *F. profunda* and its morphotypes e*longata* small, medium, and large, and variation *profunda* small and medium. The UPZ assemblage was dominant in both traps throughout the study period. In the Perdido trap the UPZ assemblage reached 78 % on average of the total coccolithophore assemblage, showing peaks in mid-summer, late autumn, and mid-winter. On the other hand, in the Coatzacoalcos trap, the UPZ assemblage accounted for 67 % of the total coccolithophore assemblage with peaks in early summer, late autumn, and early spring. The LPZ assemblages averaged 19 % in the Perdido trap, with peaks in early and late autumn and late spring. In the Coatzacoalcos trap, the LPZ assemblage showed 21 %, with peaks in late spring of 2016 and early autumn, and their average contribution increased considerably in spring 2017.

The UPZ assemblage showed higher fluxes in winter in both regions. The Perdido trap averaged 2.47 x 10^9 ± 0.89 x 10^9 coccoliths per $m^{-2}d^{-1}$ and 1.45 x 10^9 ± 0.97 x 10^9 coccoliths per $m^{-2}d^{-1}$ to Coatzacoalcos. The LPZ assemblage in Perdido recorded an average flux of 0.54 x 10^9 ± 0.24 x 10^9 coccoliths per m^{-2} d^{-1}, while in Coatzacoalcos averaged 0.33 x 10^9 ± 0.28 x 10^9 coccoliths per m^{-2} d^{-1} (Fig 6 A). The UPZ/LPZ ratios showed the highest values in winter in the Perdido trap in comparison to the Coatzacoalcos trap that showed a higher ratio in early summer, and a second peak in late autumn and early winter (Fig 6 B).

Fig 6. Seasonality of upper and lower photic zone for the Perdido and Coatzacoalcos traps. Upper Photic Zone assemblages: fluxes (blue bars) and relative abundances (blue lines with dots). Low Photic Zone assemblages: fluxes (dark blue bars) and relative abundances (dark blue lines with dots) respectively A). UPZ taxa groups the following taxa *E. huxleyi, G. oceanica, G. muellerae, Umbillicosphaera sp., Rabdosphaera sp*., and *Umbellosphaera;* and for the LPZ *G. flabellatus* and *F. profunda var profunda* and *elongata.* The UPZ/LPZ ratio (dark blue bars), and photosynthetic available radiation (mol Q m^{-2} d^{-1}) (orange solid line) B).

Relationship between environment and coccolithophores

A Spearman correlation analysis was done to identify the relationship between environmental variability and total coccolith fluxes and the "most common taxa" fluxes. The Perdido trap did not show significant values ($p< 0.05$) between any environmental variable and total coccolith flux. While in the Coatzacoalcos trap, positive correlations were observed with Mixed Layer Depth (MLD), Geostrophic Speed (GOS), and negative correlations with Photosynthetically Available Radiation (PAR), Sea Surface Temperature (SST), and Sea Surface Salinity (SSS). In the Perdido trap, the fluxes of *E. huxleyi* type A only correlate negatively with Sea Level Anomaly (SLA), while in the Coatzacoalcos trap it correlates positively with MLD and SLA and negatively with PAR, SST, and SSS. Fluxes of *G. oceanica* correlate positively with MLD and CHL and negatively with PAR and SSS in the Perdido trap, while in Coatzacoalcos, it correlates positively with MLD, GOS, CHL, and negatively with PAR. In general, the fluxes of *Florisphaera profunda* (including *profunda* and *elongata* variations) are positively correlated to SLA and SST and negatively to GOS in the Perdido trap, while in Coatzacoalcos, it is positively correlated to MLD and GOS and negatively with PAR. Other coccoliths did not show significant correlations with environmental variables (Fig 7).

Fig 7. Spearman correlation matrix. It shows the relationship between environmental parameters (bold text) and total coccolith flux = Total Flux*,* the main taxa: *Emiliania huxleyi* type A = *E. hux* (A), *Gephyrocapsa oceanica* = *G.*

oce, Florisphaera profunda var. *elongata* small = *F. prof* (e s), *F. profunda* var. *profunda* small = *F. prof* (p s), *Umbellosphaera tenuis* = *U. ten*, *Gladiolithus flabellatus* = *G. flab, F. profunda* var. *elongata* medium = *F. prof* (e m), and Other coccoliths of which some species are shown: *E. huxleyi* type B = *E. hux* (B), *Umbellosphaera irregularis* = *U. irr*, *Umbilicosphaera sibogae* = *U. sib, Syracosphaera pulchra* = *S. pul*, *F. profunda* var. *elongata* large = *F. prof (e l), F. profunda* var. *profunda* medium = *F. prof* (p m). White circles represent the species of coccoliths associated with the Upper Photic Zone, black circles represent the Low Photic Zone. Blue colors are positive correlations, and red is the negative correlation, gray squares represent significative correlation (p<0.05).

A principal component analysis using environmental data shows that 89.6 % of the total variance within the data set is explained by the two first components, Mixed Layer Depth, and Sea Level Anomaly. The first component (PC1) explains 73.6 % of the variance and shows positive high loadings mainly with MLD, representative of physical parameters that change with water depth seasonally. The second component (PC2) SLA explains 16.0 % of the variance, is associated with sea level variations produced by cyclonic and anticyclonic eddies and is positively correlated with high PAR and negatively correlated with precipitation (Table 4). Furthermore, the PCA shows that the samples can be grouped into four groups, which denote the season of the year. Winter and summer show a clear separation, while spring and autumn can be considered transitional seasons. The summer group includes samples P1 - P5 and P21 for the Perdido trap and samples C2 - C6 for the Coatzacoalcos; the autumn group included the samples P6 – P10 and C7 – C11; winter group included P11- P15 and C12 - C16, finally, the spring group P16 - P20 and C1 and C17 – C21 (Fig 8).

Table 4. Principal component factors loadings of environmental parameters.

	Component loadings								
Variable	PC 1	PC 2	PC 3	PC 4	PC 5	PC 6	PC 7	PC 8	PC 9
MLD	0.8	0.4	0.4	0.0	-0.1	-0.1	0.0	0.0	0.0
SLA	0.0	0.0	0.1	0.0	0.0	0.1	-0.3	0.9	0.1
GOS_SPEED	0.0	0.0	-0.1	0.0	0.2	0.2	-0.5	-0.2	0.8
WND_SPEED	0.1	0.3	-0.1	0.3	0.8	0.1	0.3	0.0	-0.1
PRECIPITATION	0.1	-0.6	0.5	0.6	0.0	0.0	0.0	0.0	0.0
PAR	-0.6	0.6	0.4	0.3	-0.2	-0.1	0.0	0.0	0.1
SST	-0.2	-0.2	0.6	-0.6	0.4	-0.1	0.1	0.0	0.0
SSS	0.0	0.0	0.1	-0.1	-0.2	0.9	0.3	0.0	0.0
CHL	0.0	-0.1	-0.1	0.0	-0.1	-0.3	0.7	0.2	0.6
Variance explained by components	2.3	1.2	0.9	0.5	0.8	1.0	0.7	0.8	0.8
Percent of total variance explained	73.6	16.0	5.7	2.4	1.2	0.5	0.3	0.2	0.1

Fig 8. Principal components analysis of environmental parameters. Mixed Layer depth = MLD, sea surface temperature = SST, photosynthetically available radiation = PAR, sea level anomaly = SLA, Wind-speed = WND_S, Precipitation = PREC, Geostrophic speed = GOS, and chlorophyll = CHL. Samples are ordinated as a function of the year's seasons: to the Perdido trap = P (dots) and for the Coatzacoalcos trap = C (squares).

Discussion

The Perdido and Coatzacoalcos traps showed high seasonality in the coccolith fluxes, with maximum values in winter that decreased towards the spring and early summer of 2017. The coccolith assemblages observed in this study reflect the seasonal changes in oceanographic and atmospheric conditions that affect the Gulf of Mexico. The variability and the magnitude of the coccolith fluxes and oceanographic processes that affected them are discussed in the following sections.

Seasonal variation and magnitude of coccolith fluxes

The coccolith fluxes of the Perdido and Coatzacoalcos traps in the GOM are in the same order of magnitude compared to other areas in the Atlantic Ocean, but they are slightly higher than those recorded in the Mediterranean Sea and the California Current system (Table 5.) In general, changes in primary productivity in the surface waters are well aligned with the reported seasonal variation of the total coccolith fluxes. As recorded in

the North Atlantic, the coccolith fluxes are affected mainly by sea surface temperature seasonal changes and mesoscale eddies that affect the primary productivity [65, 66]. While in the Tropical North Atlantic Stronger stratification conditions influenced by the intertropical convergence zone during summer and autumn result in maximum coccolith fluxes [11]. As mentioned earlier oceanographic and atmospheric processes contribute to the production of coccolithophores in the photic zone, and they are transported mainly in the marine snow and fecal pellets since coccoliths are too small to sink on their own through the water column [2, 3, 39], while in regions closer to the coast, the contribution of dust from wind and rainfall runoff are the main mechanisms for sinking coccoliths to the ocean floor [67, 68].

Table 5. Comparison of maximum coccolith fluxes in different regions.

Region / Author	Geographical position (Lat/Long)	Study period	Max flux rec (coccoliths
Northeastern Atlantic Ziveri et al. (2000a)	48°N, 21° W	April 1989- April 1990	>3.2 x 1
Northeastern Atlantic Broerse et al. (2000b)	34°N 21°W (NABE-34)	April 1989-April 1990	7.5 x 10
	48°N 21°W (NABE-48)		3.2 x 10
North Atlantic Knappertsbusch & Brummer, (1995)	47°N 20°W	18 May 1990-10 June 1990	3.6 x 10
			2.3 x 10
North Atlantic Haidar et al. (2000)	31°N 64°W	February 1992-January 1993	>2.5 x1
Tropical North Atlantic Guerreiro et al. (2017)	12°N 49°W (M4)	October 2012 to November 2013	4.2 x 10
	14°N 37°W (M2)		1.5 x 1
Northeastern Arabian Sea Andruleit et al. (2000)	24°35.9' N 65°35.3' W (WPT)	October 1993-January 1995	4 x 10^9
	24°45.6' N 65°48.7' W (EPT)	May 1995-December 1996	5.4 x 10

Our results in the GoM show the maximum fluxes in winter in both regions associated with the mixed layer depth during this period. However, the magnitude of total coccolith fluxes is different in each region. For example, the fluxes in the Perdido trap during spring 2017 (samples 18-20) averaged 2.2 x 10^9 coccolith m^{-2} d^{-1}, whereas the Coatzacoalcos trap averaged 0.08 x 10^9 coccolith m^{-2} d^{-1}. This difference could be due to mixed layer depth, sea level anomaly, and rainfall (Fig 2 B and C), which may play an important role in the magnitude of total fluxes and the species composition for each region. The mixed layer is influenced by seasonal changes (wind stress) that contribute to nutrient injection in the euphotic layer and has revealed a regionalization of the deep-water region based on the recurrent total chlorophyll distribution patterns during winter using recent observational data and coupled physical-biogeochemical models of the GoM [28]. In addition, on the continental slope, the control exerted by different oceanographic processes, such as entrainment, upwelling, river plumes, and cross-shelf transport, enhances the input of nutrients to these regions and sustains slightly higher primary productivity in these regions [69].

Environmental factors that affect the sinking coccolith fluxes in the Perdido and Coatzacoalcos

The seasonal variations in coccolith fluxes cannot be easily explained by environmental variations as both locations are influenced by mesoscale phenomena such as cyclonic and anticyclonic eddies that modulate the thermohaline properties of the upper layer and the biogeochemical processes that take place in these surface waters. These differences in the magnitude of fluxes between the Perdido and Coatzacoalcos traps could be explained, in part, by the MLD deepening down to 70 m at the location of the Perdido trap during winter. In contrast, for the rest of the year, the MLD is between 10 to 30 m depth (Fig 2 B) and is probably further affected by the interaction with the Poseidon anticyclonic eddy (April 2016-July 2017) which is reflected in the variations of the SLA (Fig 2 C), resulting in a strong stratification of the column water and deepening of the nitracline [70]. The Perdido region is periodically affected by the remnant structures of anticyclonic eddies detached from the Loop Current that propagate westwards to the interior of the Gulf [71, 72]; when these anticyclonic eddies arrive at the Tamaulipas continental shelf (western continental platform) the border of these eddies sweep over this shelf and

advect organic carbon and nutrient-rich waters offshore, forming large filaments that usually extend for 100 to 200 km offshore [73]. This phenomenon is reflected in the surface chlorophyll image captured in mid-winter (Fig. 9 B). In contrast to the Coatzacoalcos region, the MLD remains above 30 m depth throughout the period (Fig. 2 B); however, this should add to the importance of the interaction between the cyclonic semi-permanent eddy and the shelf region [23] and upwelling processes along the eastern margin of the Bay of Campeche [74] to explain the chlorophyll productivity patterns observed. When these cyclonic eddies interact with the continental platform, they sweep over the Campeche Tabasco shelf, advecting coastal nutrients offshore, seasonally impacted by freshwater inputs from the largest river system in the southern Gulf of Mexico, the Grijalva-Usumacinta River complex, resulting in chlorophyll plumes and filaments extending tens to hundreds of km offshore [29] in early summer (Fig 9 D). In general, in areas influenced by anticyclonic structures (like the Perdido region), the downwelling increases the upper ocean stratification and deepens the pycnocline. In contrast, in the cyclonic eddies (like the Coatzacoalcos region), the shoaling of the pycnocline brings nutrients closer to the sun-lit surface ocean [19, 21, 71, 73], as shown by the variability of the SLA (Fig 2 C). The deepening MLD during winter can be further explained by the mechanical forcing induced by wind stress [75]. Furthermore, during winter, the GoM is affected by northerly winds, also known as “Nortes”, that cool down the surface waters and deepen the mixed layer [31, 32], injecting nutrients into the euphotic layer and thereby increasing the chlorophyll concentrations [28]. Moreover, at the beginning of the study period, the passage of tropical storm Danielle (June 19 to June 21) and category 1 hurricane Earl (2 to 6 August) through the southern GoM further affected the surface ocean conditions in the southern GoM. Tropical storm Daniel appears to be reflected by the high flux of the assemblages of the LPZ captured in the first cup of the Coatzacoalcos trap (Fig. 6 A). All these processes show a seasonal pattern. For example, the “Nortes” occurs in winter, while river discharges from Mississippi-Atchafalaya and Bravo rivers peaks during the spring to early summer in the Perdido region. On the other hand, in the Coatzacoalcos region where the Grijalva-Usumacinta River system flows into the GoM, the highest inputs are observed from summer into autumn rainy season [29, 76].

Fig 9. Spatial and temporal variability of sea surface chlorophyll in the GoM. The black circles show the catchment area of each sediment trap. Panel A) shows the average of the dataset for 11/25/2016 to 12/12/2016 (late autumn), panel B) the average from 12/31/2016 to 1/17/2017 (middle winter), panel C) shows the average from 5/24/2017 to 6/10/2017 (late spring), and Panel D) shows the average from 6/29/2017 to 7/16/2017 (early summer). Each panel represents an average of 18 days at 4 x 4 km spatial resolution. https://oceancolor.gsfc.nasa.gov/l3/.

Variability of coccolithophore assemblages

*Emiliania huxley*i is the most abundant coccolithophore in all the oceans, occurring at a relative abundance of 60-80%; it is one of the most euryhaline and eurythermal species [2] (Table 5). *G. oceanica,* which may also be dominant in warm marginal seas [77] and also found in upwelling areas like the Northeastern Arabian Sea, is associated with nutrient injection during monsoon periods [78]. In the GoM the high abundance of *E. huxleyi* and *G. oceanica* was associated with the seasonality of mixed layer, resulting in the availability of nutrients in the photic zone. On the other hand, *Florisphaera profunda* is a species characteristic of the lower photic zone that occurs at low light intensities (~1% light) and high nutrient concentrations [44, 50]. Our results show an increase in the relative abundances of *F. profunda* var. *profunda* small (25-48%) and *F. profunda* var. *elongata* small (15-30%) from the middle of spring 2017 to the end of the sampling period (samples 18-21) that coincides with a peak of the precipitation (11 mm d^{-1}) to Coatzacoalcos trap. Precipitation could have favored low-light conditions and input nutrients and increased relative abundances of this species due to the discharges of the Coatzacoalcos River. A similar phenomenon occurred in the Equatorial North Atlantic under conditions where the low-light and deep nutricline dwelling favored the dominance of *F. profunda* and *G. flabellatus* were most abundant during autumn 2012 reaching ~74% of assemblages [11]. Although species categorized as “Other coccoliths” are less abundant, they play a significant role ecologically in terms of richness and diversity and could be associated with seasonal changes in photosynthetically active radiation, sea surface temperature and salinity. Pariente (13)

reported that *Umbellosphaera irregularis*, *U. tenuis*, and *F. profunda* were dominant during October 1990 and *E. huxleyi* and *F. profunda* during March 1991, and their higher coccolithophores concentration was associated with a warm-core eddy. The High kinetic energy of anticyclonic eddies (>0.5 m/s^{-1}) has the potential to retain plankton communities ranging from weeks to months [79-81] affecting the nutrient levels in the euphotic zone [82] and, therefore, the phytoplankton and zooplankton biomass inside cyclonic and anticyclonic eddies [83, 84].

Oceanographic implications of Upper and Lower photic zone assemblages

The dominance of species associated with the upper photic zone over those of the lower photic zone shows the prevalence of oligotrophic conditions in the depth ocean of the GoM. Since in oligotrophic regions, the phytoplankton groups are limited by nutrient availability in the upper euphotic zone and light intensity in the lower euphotic zone [85]. Cortés, Bollman (50) reported from living coccolithophores at the Hawaii Ocean Time-series station that the UPZ assemblages were mostly influenced by temperature and the availability of phosphate. In contrast, the LPZ assemblages are most likely limited by light and nitrate. In both regions on the GoM that we studied, it was observed that the LPZ assemblages recorded high relative abundances that coincided with the rainy season. The high relative abundances recorded in the LPZ assemblages to the Coatzacoalcos trap during late spring 2016 (Fig 6 A, sample 1) could be the result of the passage of the Danielle tropical storm and during late summer-early autumn reflected the freshwater runoff of Coatzacoalcos River described by GonzáLez-Ramírez and Parés-Sierra (86), thereby limiting light penetration to the LPZ, which is reflected in a slight increase in the relative abundances of the LPZ assemblages (Fig 6 A). While the significant decline in upper and lower photic zone taxa during the spring of 2017 in both regions (more evident in Coatzacoalcos) appears to respond to the confluence of seasonal coastal currents and wind stress that results in high chlorophyll concentrations on the sea surface proposed by Martínez-López and Zavala-Hidalgo (29). The higher UPZ/LPZ ratio during winter in comparison to the rest of the study period (Fig 6 B) in the Perdido region suggests an increase in nutrient entrainment into the euphotic zone due to a deepening of the MLD as a result of wind mixing. The lowest ratios during summer suggest a higher stratification of the surface waters and a deeper nitracline [52] as shown in the

PAR variation (Fig 6 B). In contrast, during early summer in the Coatzacoalcos region, higher values of the UPZ/LPZ ratio may be evidence of the presence of the core of the Campeche cyclonic eddy (Fig 2 C) with enhanced mixing and higher nutrient availability in the upper photic zone. Guerreiro, Baumann (11), with a sediment trap study, documented the occasional sharp rise in the UPZ/LPZ ratio at station M4 (12°N 49°W, Amazon influenced), indicating that the nutricline was briefly shallower, although this is a zone-dominated by the LPZ assemblages, during these events, there is a fast production by the opportunistic coccolithophore in response to the higher nutrient availability. In other sediment traps deployed in the Cape Blanc region, the assemblage was dominated by UPZ species and the highest abundances was associated with the upwelling system off NW Africa [87] and the Bay of Bengal by Stoll, Arevalos (54), and the South of the California Current [88], also affected by coastal upwellings. This is reflected in the shallowed of the nutricline and low fluxes of the LPZ assemblages [52, 89].

The canonical correspondence analysis (CCA) shows a correlation between coccolith fluxes and environmental variables in the Perdido and Coatzacoalcos traps, where the mixed layer depth (MLD), sea level anomaly (SLA), and geostrophic speed (GOS) explain 92 % of the variance (Fig 10, Table 6). The CCA is a multivariate technique that analyzes the relationship between coccolith fluxes and environmental variables, assuming species respond to a standard set of underlying environmental gradients. The ordination axes facilitate the interpretation of CCA results. The eigenvalues and species-environment correlation coefficients provide quantitative measures of the importance of each axis and the strength of the relationship between species and environmental variables [64]. Our results show that during winter (lilac polygon), the mixed layer deepens due to wind forcing [31], promoting the injection of nutrients to the upper photic zone [28, 69], favoring the generalist species (UPZ taxa) such as *E. huxleyi* and *G. oceanica,* both of which have a cosmopolitan distribution showing their high abundances in nutrient-rich environments and continental shelves [2, 90]. In other oligotrophic regions, such as the Mediterranean Sea, the dominance of *E. huxleyi* has been reported where the SST and precipitation are environmental parameters associated with the seasonality of fluxes [67, 91, 92]. Our results show that the Sea surface temperature has a marked seasonality oriented towards the spring (green polygon) and summer (beige

polygon), indicating a greater stratification of the water column and nutrient-depleted surface water. Under these conditions, ***k**-strategy* species inhabiting the upper photic zone (*U. tenuis, D. tubifera*, and *Rhabdosphaera* spp.) flourish as documented in a plankton study from the Southern Mediterranean Sea [93, 94]. On the other hand, our results show that the LPZ assemblages (*F. profunda* and *G. flabellatus*) depend on the photosynthetically available radiation (PAR) (p=0.001) and to a lesser extent with Precipitation (p=0.06). Both species have been recorded as restricted to light in the lower euphotic zone in the tropical and subtropical oceans [51, 95, 96]. The inverse correlation (-0.57) between *E. huxleyi* and *F. profunda* (only with *Elongata* medium) suggests a seasonal marked stratification in the Perdido trap, while in the Coatzacoalcos, the correlation between this species was positive (around 0.5 for LPZ assemblages) (Fig 7), suggesting greater mixing in the water column and a coccolithophore production throughout the water column [68, 95].

The geostrophic velocity and sea level anomaly, associated with ocean surface topography caused by mesoscale phenomena such as cyclonic and anticyclonic eddies usually impact the transport and mixing in the column water [71, 97, 98], Our results clearly show the importance of the MDL controlling the nutrient availability in the upper photic zone and the primary production that modulates the magnitude of coccolith fluxes in both study regions.

Fig 10. Ordination diagram of the canonical correspondence analysis (CCA) for the Perdido and Coatzacoalcos traps. Performed with the environmental variables (MLD, SLA, GOS, WND_S, PREC, PAR, SST, SSS, CHL) that were averaged over the 18 days for each cup opening (July 2016 to June 2017) and the principal coccolith fluxes: *Emiliania huxleyi* type A = *E. hux* (A), *Gephyrocapsa oceanica* = *G. oce, Florisphaera profunda elongata* small = *F. prof* (e s), *F. profunda profunda* small = *F. prof* (p s), Umbellosphaera tenuis = U. ten, *Gladiolithus flabellatus* = *G. flab*, *E. huxleyi* type A = *E. hux* (B), *F. profunda elongata medium* = *F. prof* (e m), and Others coccoliths group *Umbellosphaera irregularis* = *U. irr, Umbilicosphaera sibogae* = *U. sib, Syracosphaera pulchra* = *S. pul, Calciosolenia brasiliensis* = *C. Bra, F. profunda var. elongata* large = *F. prof* (e l)*, Discosphaera tubifera* = *D.tub, F. profunda profunda medium* = *F. prof* (p m)*, F.profunda var. Rhinocera* = *F.* (rhi). The colors of polygons indicate the seasons of the year and are formed by each of the samples (points).

Ecological implications

Coccolith fluxes in the sediment traps reflect the primary productivity and the related physico-chemical processes. In the Perdido region, the mixed layer depth deepening results in nutrient enrichment of the surface waters, increasing biomass and primary production. In contrast, in the Coatzacoalcos region, the Nortes hardly affect the deepening of the MLD, which most likely leads to a lesser injection of nutrients in the euphotic layer and consequently, to a lower PP and biomass [28, 69]. This process triggers nutrient competition between the different phytoplankton groups, increasing the opportunistic species or type *r* selection [99]. Our results show that the abundance of *E. huxleyi* and *G. oceanica* increased during these events, especially in the Perdido region. This increase in chlorophyll concentration (Fig 9 D) could reflect the increase in diatoms and coccolithophores as reported by Hernández-Becerril, García-Reséndiz (14), most probably inducing a synecological competition between both groups as described in the Northern Arabian Sea [100]. Although we did not analyze other phytoplanktonic groups in this work, Linacre, Lara-Lara (101) recorded an increase in the picoplankton biomass, mainly Prochlorococcus, Synechococcus, and pico-eukaryotes during winter in the Southern GoM, that were strongly associated with the mesoscale dynamics that modulated the hydrographic conditions of the surface mixed layer. In oligotrophic ecosystems, during stratification periods, the limited nutrients available in the euphotic zone are recycled more rapidly, giving smaller cells a competitive advantage over larger ones [102, 103]. Consequently, Pico and nannoplankton, such as coccolithophores, dominate these systems and form the foundation of the food chain, as low nutrient levels do not restrict coccolithophores growth [104]. Therefore, it is very likely that during these events, the competition between these groups, as well as the ecological succession contributes to the stability of the ecosystem (favoring *k*-type species) during summer [105]. Observations have shown that when resources are extremely limited (low nutrient conditions), coccolithophores can absorb organic compounds by mixotrophy [106, 107], a strategy that may play an important role in oligotrophic systems such as the GoM. The lowest fluxes recorded in the Coatzacoalcos trap potentially reflect the limited nutrient availability [29] and overall primary productivity [28, 30] in the southern GoM during the spring-summer stratification of the surface waters [28].

The complexity of understanding the coccolith fluxes in the Gulf of Mexico depends not only on environmental factor measurement here but also on the interaction of the mesoscale eddies and fronts that greatly impact lateral transport and turn the trajectories of sinking particles, resuspension of sediment, lateral advection and others, but they do help greatly to comprehend the dynamics of coccolith exporting in the Southwestern part of the Gulf of Mexico.

Conclusion

The present study documents the seasonal variability of coccolith fluxes in the Perdido region in the western GoM and Coatzacoalcos regions in the southwestern GoM and analyzed the most likely environmental parameters controlling the flux.

- The Perdido region shows an assemblage composed of 47 species of coccoliths, while Coatzacoalcos shows 56 species throughout the study period. The ecological index shows higher richness and diversity in the Coatzacoalcos region than in the Perdido region; both regions presented low evenness, suggesting the dominance of a few species.
- Three species dominated the composition in both areas, although with different relative abundance. *E. huxleyi* reached an average of 61 % in the Perdido region, while in Coatzacoalcos it reached 46 %. *G. oceanica* accounted for 10 % and 13 % in the Perdido and Coatzacoalcos regions, respectively; this species reflected a fast ecological response to intermittent nutrient input promoted by wind forces and vertical mixing. *F. profunda* reached 17 % in the Perdido and 25 % in Coatzacoalcos, respectively. High abundances of *F. profunda* were associated with deep nutricline, and low abundances with shallow nutricline as a result of mixed layer depth variation.
- We further observed higher abundances of this species associated with extreme precipitation events after tropical storm Danielle (19- 21 June 2016), in September-October 2016, most likely due to attenuated light in the upper photic zone that favored its population growth of this low light adapted species.

- The Other coccoliths group, with low mean relative values, represented 6 % in Perdido and 10 % in the Coatzacoalcos region.
- The upper photic assemblage dominated throughout the study period in both regions. The UPZ/LPZ ratios follow the variability of the nutricline; the highest ratios were related to a deeper mixed layer and higher coccolith fluxes during winter in both regions. In the Coatzacoalcos region, the high UPZ/LPZ values during early summer were most likely related to the cyclonic eddy.
- The seasonality is clearly expressed in high coccolith fluxes that occur in winter, decreasing into the spring and summer. The Perdido region trap showed slightly higher fluxes max 4.3 x 10^9 coccoliths per $m^{-2}d^{-1}$, in February 2017, with an annual average of 3.1 x 10^9 ± 0.89 x 10^9 coccoliths per $m^{-2}d^{-1}$, followed by a second peak during autumn (4.20 x 10^9 coccoliths per $m^{-2}d^{-1}$). The Coatzacoalcos region trap shows maximum fluxes of 3.8 x 10^9 coccoliths per $m^{-2}d^{-1}$ in January and an annual average of 1.9 x 10^9 ± 1.13 x 10^6 coccoliths $m^{-2}d^{-1}$. Moderate fluxes in summer-autumn reflect upper ocean stratification and the low nutrient availability in the upper photic zone, implying the importance of that mixotrophy to explain these fluxes.
- Our findings suggest that mixed layer dynamics associated with the Northern winds during winter and the mesoscale anticyclonic eddy (Poseidon) to the Perdido region and semi-permanent cyclonic eddy (Campeche Bay) to Coatzacoalcos modulated the coccolith fluxes variability.

Acknowledgments

The authors are grateful to all the people involved in the Gulf of Mexico Research Consortium (CIGOM, https://cigom.org/). We thank Dr. Fernando Aguirre-Bahena (deceased) for his dedication, effort, and planning of the installation of the deployment used in this work. As well as the collaboration of the crew of the Oceanographic Research Vessel “Rio Hondo” of the Mexican Navy and collaboration of the CICESE Wave group for the installation and recovery of the sediment traps. We also thank the CANEK group for the recovery of the Perdido trap. Felipe

García-Romero was supported by a CONAHCYT PhD fellowship. This study was conducted using information from the E.U. Marine Service; https://data.marine.copernicus.eu/products.

Author Contributions

Conceptualization: Felipe García-Romero.

Data curation: Felipe García-Romero, Amaru Márquez-Artavia.

Formal Analysis: Felipe García-Romero.

Funding acquisition: J. Rubén Lara-Lara.

Investigation: Felipe García-Romero, J. C. Herguera-García, Jörg Bollmann, M. Y. Cortés, J. Rubén Lara-Lara.

Methodology: Felipe García-Romero, Jörg Bollmann, M. Y. Cortés, Amaru Márquez-Artavia.

Project administration: J. Rubén Lara-Lara, J. C. Herguera-García.

Resources: J. Rubén Lara-Lara, J. C. Herguera-García.

Software: Felipe García-Romero, Amaru Márquez-Artavia.

Supervision: J. C. Herguera-García, Jörg Bollmann, M. Y. Cortés, J. Rubén Lara-Lara.

Validation: Felipe García-Romero, J. C. Herguera-García, Jörg Bollmann, M. Y. Cortés.

Visualization: Felipe García-Romero, M. Y. Cortés, Jörg Bollmann, J. C. Herguera-García, J. Rubén Lara-Lara.

Writing – original draft: Felipe García-Romero.

Writing review & editing: Felipe García-Romero, Jörg Bollmann, J. C. Herguera-García, M. Y. Cortés, Amaru Márquez-Artavia, J. Rubén Lara-Lara.

References

1. Westbroek P, Brown Christopher W, Bleijswijk Jv, Brownlee C, Brummer GJ, Conte M, et al. A model system approach to biological climate forcing; the example of Emiliania huxleyi. In: de Baar HJW, Suess E, editors. Ocean carbon cycle and climate change. 81993. p. 27-46.
2. Winter A, Siesser WG. Coccolithophores. Cambridge: Cambridge University Press; 1994.
3. Honjo S. Coccoliths: Production, Transportation and Sedimentation. Marine Micropaleontology. 1976;1:65-79.
4. Honjo S. Material fluxes and modes of sedimentation in the mesopelagic and bathypelagic zones. Journal of Marine Research. 1980;38(1).
5. Honjo S, Doherty KW. Large aperture time-series sediment traps; design objectives, construction and application. Deep Sea Research Part A: Oceanographic Research Papers. 1988;35(1):133-49.
6. Knappertsbusch M, Brummer GJA. A sediment trap investigation of sinking coccolithophorids in the North Atlantic. Deep Sea Research Part I: Oceanographic Research Papers. 1995;42(7):1083-109. doi: https://doi.org/10.1016/0967-0637(95)00036-6.

7. Broerse ATC, Ziveri P, van Hinte JE, Honjo S. Coccolithophore export production, species composition, and coccolith - $CaCO_3$ fluxes in the NE Atlantic (34°N 21°W and 48°N 21°W). Deep Sea Reserch II. 2000;47:1877-905.
8. Haidar AT, Thierstein HR, Deuser WG. Calcareous phytoplankton standing stocks, fluxes and accumulation in Holocene sediments off Bermuda (N. Atlantic). Deep-Sea Research Part II. 2000;47:1907-38.
9. Klaas C, Archer DE. Association of sinking organic matter with various types of mineral ballast in the deep sea: implications for the rain ratio. Global Biogeochemical Cycles. 2002;16:GB1116.
10. Hayat S, Skampa E, Gogou A, Stavrakakis S, Parinos C, Triantaphyllou M. Seasonal Variability in Present-Day Coccolithophore Fluxes in Deep Eastern Mediterranean Sea: A Multi-Year Study (2015–2017) of Coccolithophore Export in SE Ionian Sea at 4300 m Depth. Journal of Marine Science and Engineering. 2022;10(11):1761. doi: 10.3390/jmse10111761.
11. Guerreiro CV, Baumann K-H, Brummer G-JA, Fischer G, Korte LF, Merkel U, et al. Coccolithophore fluxes in the open tropical North Atlantic: influence of thermocline depth, Amazon water, and Saharan dust. Biogeosciences. 2017;14:4577-99. doi: 10.5194/bg-14-4577-2017.
12. Gaarder KR, Hasle GR. Coccolithophorids of the Gulf of Mexico. Bulletin of Marine Science. 1971;21(2):519-44.
13. Pariente V. Coccolithophores of the Gulf of Mexico and their relationship to water-column properties [Ph.D.]. Ann Arbor: Texas A&M University; 1997.
14. Hernández-Becerril dU, García-Reséndiz J, Salas de Leon D, Monreal-Goméz M, Poillon M-, JAldeco-Ramírez. Nanoplankton fraction in the phytoplankton structure in the southern Gulf of Mexico (April 2000). Ciencias Marinas. 2008;34(1):77-90.
15. Agbali A. Investigations of the Ecology of Calcareous Nannoplankton and Nannofossils in the North-East Gulf of Mexico to Help Establish a Baseline for Environmental Impact Studies [Doctor]: FLORIDA STATE UNIVERSITY; 2014.
16. Cruz JW, S. W. ; Young, J. R. First observation of Navilithus altivelum in the Gulf of Mexico. Journal of Nannoplankton Research. 2014;34:27-9.
17. Cruz J, Wise SWJ, Parker W, Young JR. Distribution of NE Gulf of Mexico nannoplankton assemblages following the Macondo Well blowout: August–November 2011–2013. Journal of Nannoplankton Research. 2019;S4:39-54. doi: DOI: https://doi.org/10.58998/jnr2071.
18. Baumann K-H, Boeckel B. Spatial distribution of living coccolithophores in the southwestern Gulf of Mexico. Journal of micropaleontology. 2013;32:123-33.
19. Elliott BA. Anticyclonic Rings in the Gulf of Mexico. Journal of Physical Oceanography. 1982;12(11):1292-309. doi: 10.1175/1520-0485(1982)012<1292:aritgo>2.0.co;2.
20. Oey LY, Ezer T, Lee Hc. Loop Current, Rings and Related Circulation in the Gulf of Mexico: A Review of Numerical Models and Future Challenges. Geophysical monograph. 2013;161:31-56.
21. Weisberg RH, Liu Y. On the Loop Current Penetration into the Gulf of Mexico. Journal of Geophysical Research: Oceans. 2017;122(12):9679-94. doi: doi:10.1002/2017JC013330.
22. Sturges W. The annual cycle of the western boundary current in the Gulf of Mexico. Journal of Geophysical Research: Oceans. 1993;98(C10):18053-68. doi: 10.1029/93jc01730.
23. Pérez-Brunius P, García-Carrillo P, Dubranna J, Sheinbaum J, Candela J. Direct observations of the upper layer circulation in the southern Gulf of Mexico. Deep Sea Research Part II: Topical Studies in Oceanography. 2013;85:182-94. doi: https://doi.org/10.1016/j.dsr2.2012.07.020.
24. Vázquez De La Cerda AM, Reid RO, DiMarco SF, Jochens AE. Bay of Campeche Circulation: An Update. Circulation in the Gulf of Mexico: Observations and Models2005. p. 279-93.
25. Durán-Campos E, Salas-de-León DA, Monreal-Gómez MA, Coria-Monter E. Patterns of chlorophyll-a distribution linked to mesoscale structures in two contrasting areas Campeche Canyon and Bank, Southern Gulf of Mexico. Journal of Sea Research. 2017;123:30-8. doi: https://doi.org/10.1016/j.seares.2017.03.013.
26. Müller-Karger FE, Walsh JJ, Evans RH, Meyers MB. On the seasonal phytoplankton concentration and sea surface temperature cycles of the Gulf of Mexico as determined by satellites. Journal of Geophysical Research: Oceans. 1991;96(C7):12645-65. doi: https://doi.org/10.1029/91JC00787.
27. Biggs DC, Müller-Karger FE. Ship and satellite observations of chlorophyll stocks in interacting cyclone-anticyclone eddy pairs in the western Gulf of Mexico. Journal of Geophysical Research: Oceans. 1994;99(C4):7371-84. doi: https://doi.org/10.1029/93JC02153.
28. Damien P, Pasqueron de Fommervault O, Sheinbaum J, Jouanno J, Camacho-Ibar VF, Duteil O. Partitioning of the Open Waters of the Gulf of Mexico Based on the Seasonal and Interannual Variability of Chlorophyll Concentration. Journal of Geophysical Research: Oceans. 2018;123(4):2592-614. doi: https://doi.org/10.1002/2017JC013456.
29. Martínez-López B, Zavala-Hidalgo J. Seasonal and interannual variability of cross-shelf transports of chlorophyll in the Gulf of Mexico. Journal of Marine Systems. 2009;77(1):1-20. doi: https://doi.org/10.1016/j.jmarsys.2008.10.002.

30. Pasqueron de Fommervault O, Perez-Brunius P, Damien P, Camacho-Ibar VF, Sheinbaum J. Temporal variability of chlorophyll distribution in the Gulf of Mexico: bio-optical data from profiling floats. Biogeosciences. 2017;14(24):5647-62. doi: 10.5194/bg-14-5647-2017.
31. Muller-Karger FE, Smith JP, Werner S, Chen R, Roffer M, Liu Y, et al. Natural variability of surface oceanographic conditions in the offshore Gulf of Mexico. Progress in Oceanography. 2015;134:54-76. doi: https://doi.org/10.1016/j.pocean.2014.12.007.
32. Zavala-Hidalgo J, Romero-Centeno R, Mateos-Jasso A, Morey SL, Martínez-López B. The response of the Gulf of Mexico to wind and heat flux forcing: What has been learned in recent years? Atmósfera. 2014;27(3):317-34. doi: https://doi.org/10.1016/S0187-6236(14)71119-1.
33. Alvera-Azcárate A, Barth A, Weisberg RH. The Surface Circulation of the Caribbean Sea and the Gulf of Mexico as Inferred from Satellite Altimetry. Journal of Physical Oceanography. 2009;39(3):640-57. doi: https://doi.org/10.1175/2008JPO3765.1.
34. Cardona Y, Bracco A, Villareal TA, Subramaniam A, Weber SC, Montoya JP. Highly variable nutrient concentrations in the Northern Gulf of Mexico. Deep Sea Research Part II: Topical Studies in Oceanography. 2016;129:20-30. doi: https://doi.org/10.1016/j.dsr2.2016.04.010.
35. Bargu S, Justic D, White JR, Lane R, Day J, Paerl H, et al. Mississippi River diversions and phytoplankton dynamics in deltaic Gulf of Mexico estuaries: A review. Estuarine, Coastal and Shelf Science. 2019;221:39-52. doi: https://doi.org/10.1016/j.ecss.2019.02.020.
36. Knauer GA, Karl DM, Martin JH, Hunter CN. In situ effects of selected preservatives on total carbon, nitrogen and metals collected in sediment traps. Journal of Marine Research. 1984;42:445-62.
37. Karl DM, Knauer GA. Swimmers: A Recapitulation of the Problem and a Potential Solution. Oceanography. 1989;2:32-5.
38. Michaels AF, Silver MW, Gowing MM, Knauer GA. Cryptic zooplankton "swimmers" in upper ocean sediment traps. Deep Sea Research Part A Oceanographic Research Papers. 1990;37(8):1285-96. doi: https://doi.org/10.1016/0198-0149(90)90043-U.
39. Honjo S. Sedimentation of materials in the Sargasso Sea at a 5,367 m deep station. Journal of Marine Research. 1978;36(3).
40. Bairbakhish AN, Bollmann J, Sprengel C, Thierstein HR. Disintegration of aggregates and coccospheres in sediment trap samples. Marine Micropaleontology. 1999;37(2):219-23. doi: http://dx.doi.org/10.1016/S0377-8398(99)00019-5.
41. Bollmann J, Cortés MY, Haidar AT, Brabec B, Crose A, Hofmann R, et al. Techniques for quantitative analyses of calcareous marine phytoplankton. Marine Micropaleontology. 2002;44:163-85.
42. Andruleit H. Coccolithophore fluxes in the Norwegian-Greenland Sea: seasonality and assemblage alterations. Marine Micropaleontology. 1997;31:45-64.
43. Young J, Geisen M, Cros L, Kleijne A, Sprengel C, Probert I, et al. A guide to extant coccolithophore taxonomy2003 Young et al., 2003. 1-124 p.
44. Quinn P, Cortes M, Bollmann J. Morphological variation in the deep sea ocean-dwelling coccolithophore *Florisphaera profunda* (Haptophyta). Eur J Phycol. 2005;40(1):31 - 42.
45. Bollmann. Morphology and biogeography of Gephyrocapsa coccoliths in Holocene sediments. Marine Micropaleontology. 1997;29:319-50.
46. Kleijne A, Cros L. Ten new extant species of the coccolithophore Syracosphaera and a revised classification scheme for the genus. Micropaleontology. 2009;55(5):425-62. PubMed PMID: WOS:000274809400001.
47. Shannon CE, Weaver W. The mathematical theory of communication. Urbana, editor. University of Illinois Press1949.
48. Pielou EC. The measurement of diversity in different types of biological collections. Journal of Theoretical Biology. 1966;13:131-44. doi: https://doi.org/10.1016/0022-5193(66)90013-0.
49. Berger WH, Parker FL. Diversity of Planktonic Foraminifera in Deep-Sea Sediments. Science. 1970;168(3937):1345-7. doi: doi:10.1126/science.168.3937.1345.
50. Cortés MY, Bollman J, Thierstein HR. Coccolithophore ecology at the HOT station ALOHA, Hawaii. Deep-Sea Research Part II. 2001;48:1957-81.
51. Kinkel H, Baumann KH, Čepek M. Coccolithophores in the equatorial Atlantic Ocean: response to seasonal and Late Quaternary surface water variability. Marine Micropaleontology. 2000;39(1):87-112. doi: https://doi.org/10.1016/S0377-8398(00)00016-5.
52. Molfino B, McIntyre A. Precessional Forcing of Nutricline Dynamics in the Equatorial Atlantic. Science. 1990;249(4970):766-9. doi: doi:10.1126/science.249.4970.766.
53. Winter A, Rost B, Hilbrecht H, Elbrächter M. Vertical and horizontal distribution of coccolithophores in the Caribbean Sea. Geo-Marine Letters. 2002;22(3):150-61. doi: 10.1007/s00367-002-0108-8.

54. Stoll HM, Arevalos A, Burke A, Ziveri P, Mortyn G, Shimizu N, et al. Seasonal cycles in biogenic production and export in Northern Bay of Bengal sediment traps. Deep Sea Research Part II: Topical Studies in Oceanography. 2007;54(5):558-80. doi: https://doi.org/10.1016/j.dsr2.2007.01.002.
55. Poulton AJ, Holligan PM, Charalampopoulou A, Adey TR. Coccolithophore ecology in the tropical and subtropical Atlantic Ocean: New perspectives from the Atlantic meridional transect (AMT) programme. Progress in Oceanography. 2017;158:150-70. doi: https://doi.org/10.1016/j.pocean.2017.01.003.
56. Waniek J, Koeve W, Prien RD. Trajectories of sinking particles and the catchment areas above sediment traps in the northeast Atlantic. Journal of Marine Research. 2000;6(58): 983-1006. doi: doi:10.1357/002224000763485773.
57. Huang B, Liu C, Banzon V, Freeman E, Graham G, Hankins B, et al. Improvements of the Daily Optimum Interpolation Sea Surface Temperature (DOISST) Version 2.1. Journal of Climate. 2021;34(8):2923-39. doi: https://doi.org/10.1175/JCLI-D-20-0166.1.
58. Hu C, Lee Z, Franz B. Chlorophyll aalgorithms for oligotrophic oceans: A novel approach based on three-band reflectance difference. Journal of Geophysical Research: Oceans. 2012;117(C1). doi: https://doi.org/10.1029/2011JC007395.
59. Atlas R, Hoffman RN, Ardizzone J, Leidner SM, Jusem JC, Smith DK, et al. A Cross-calibrated, Multiplatform Ocean Surface Wind Velocity Product for Meteorological and Oceanographic Applications. Bulletin of the American Meteorological Society. 2011;92(2):157-74. doi: https://doi.org/10.1175/2010BAMS2946.1.
60. Mears C, Lee T, Ricciardulli L, Wang X, Wentz F. Improving the Accuracy of the Cross-Calibrated Multi-Platform (CCMP) Ocean Vector Winds. Remote Sensing. 2022;14(17):4230. PubMed PMID: doi:10.3390/rs14174230.
61. Metzger EJ, Ole Martin S, Prasad GT, Harley EH, James AC, Alan JW, et al. US Navy Operational Global Ocean and Arctic Ice Prediction Systems. Oceanography. 2014;27.
62. Frouin R, Tan J, Ramon D, Franz B, Murakami H. Estimating photosynthetically available radiation at the ocean surface from EPIC/DSCOVR data: SPIE; 2018.
63. Huffman GJ, Bolvin DT, Braithwaite D, Hsu K-L, Joyce RJ, Kidd C, et al. Integrated Multi-satellite Retrievals for the Global Precipitation Measurement (GPM) Mission (IMERG). In: Levizzani V, Kidd C, Kirschbaum DB, Kummerow CD, Nakamura K, Turk FJ, editors. Satellite Precipitation Measurement: Volume 1. Cham: Springer International Publishing; 2020. p. 343-53.
64. Braak CJF. Canonical Correspondence Analysis: A New Eigenvector Technique for Multivariate Direct Gradient Analysis. Ecology. 1986;67(5):1167-79. doi: https://doi.org/10.2307/1938672.
65. Ziveri P, Broerse ATC, van Hinte JE, Westbroek P, Honjo S. The fate of coccoliths at 48°N 21°W, Northeastern Atlantic. Deep Sea Research Part II: Topical Studies in Oceanography. 2000;47(9):1853-75. doi: https://doi.org/10.1016/S0967-0645(00)00009-6.
66. Broerse ATC, Ziveri P, van Hinte JE, Honjo S. Coccolithophore export production, species composition, and coccolith-CaCO3 fluxes in the NE Atlantic (34°N21°W and 48°N21°W). Deep Sea Research Part II: Topical Studies in Oceanography. 2000;47(9):1877-905. doi: https://doi.org/10.1016/S0967-0645(00)00010-2.
67. Triantaphyllou MV, Ziveri P, Tselepides A. Coccolithophore export production and response to seasonal surface water variability in the oligotrophic Cretan Sea (NE Mediterranean). Micropaleontology. 2004;50(Suppl_1):127-44. doi: 10.2113/50.Suppl_1.127.
68. Ziveri P, Rutten A, de Lange GJ, Thomson J, Corselli C. Present-day coccolith fluxes recorded in central eastern Mediterranean sediment traps and surface sediments. Palaeogeography, Palaeoclimatology, Palaeoecology. 2000;158(3):175-95. doi: https://doi.org/10.1016/S0031-0182(00)00049-3.
69. Salmerón-García O, Zavala-Hidalgo J, Mateos-Jasso A, Romero-Centeno R. Regionalization of the Gulf of Mexico from space-time chlorophyll-a concentration variability. Ocean Dynamics. 2011;61(4):439-48. doi: 10.1007/s10236-010-0368-1.
70. Brokaw RJ, Subrahmanyam B, Trott CB, Chaigneau A. Eddy Surface Characteristics and Vertical Structure in the Gulf of Mexico from Satellite Observations and Model Simulations. Journal of Geophysical Research: Oceans. 2020;125(2):e2019JC015538. doi: https://doi.org/10.1029/2019JC015538.
71. Vidal VMV, Vidal FV, Pérez-Molero JM. Collision of a loop current anticyclonic ring against the continental shelf slope of the western Gulf of Mexico. Journal of Geophysical Research: Oceans. 1992;97(C2):2155-72. doi: https://doi.org/10.1029/91JC00486.
72. Vidal VMV, Vidal FV, Hernández AF, Meza E, Zambrano L. Winter water mass distributions in the western Gulf of Mexico affected by a colliding anticyclonic ring. Journal of Oceanography. 1994;50(5):559-88. doi: 10.1007/BF02235424.
73. Biggs DC, Muller-Karger FE. Ship and satellite observations of chlorophyll stocks in interacting cyclone-anticyclone eddy pairs in the western Gulf of Mexico. Journal of Geophysical Research. 1994;99(C4):7371-84. doi: 10.1029/93JC02153.
74. Zavala-Hidalgo J, Gallegos-García A, Martínez-López B, Morey SL, O'Brien JJ. Seasonal upwelling on the Western and Southern Shelves of the Gulf of Mexico. Ocean Dynamics. 2006;56(3):333-8. doi: 10.1007/s10236-006-0072-3.

75. de Boyer Montégut C, Madec G, Fischer AS, Lazar A, Iudicone D. Mixed layer depth over the global ocean: An examination of profile data and a profile-based climatology. Journal of Geophysical Research: Oceans. 2004;109(C12). doi: https://doi.org/10.1029/2004JC002378.
76. González-Ramírez J, Parés-Sierra A, Cepeda-Morales J. Chlorophyll response to wind and terrestrial nitrate in the western and southern continental shelves of the Gulf of Mexico. Frontiers in Marine Science. 2023;10. doi: 10.3389/fmars.2023.1034638.
77. Okada H, Honjo S. Distribution of coccolithophores in marginal seas along the western Pacific Ocean and in the Red Sea. Marine Biology. 1975;31(3):271-85. doi: 10.1007/BF00387154.
78. Andruleit HA, Von Rad U, Bruns A, Ittekkot V. Coccolithophore fluxes from sediment traps in the northeastern Arabian Sea off Pakistan. Marine Micropaleontology. 2000;38:285 - 308.
79. Christaki U, Giannakourou A, Van Wambeke F, Grégori G. Nanoflagellate predation on auto- and heterotrophic picoplankton in the oligotrophic Mediterranean Sea. Journal of Plankton Research. 2001;23(11):1297-310. doi: 10.1093/plankt/23.11.1297.
80. Menna M, Poulain P-M, Zodiatis G, Gertman I. On the surface circulation of the Levantine sub-basin derived from Lagrangian drifters and satellite altimetry data. Deep Sea Research Part I: Oceanographic Research Papers. 2012;65:46-58. doi: https://doi.org/10.1016/j.dsr.2012.02.008.
81. Bello-Fuentes FJ, García-Nava H, Andrade-Canto F, Durazo R, Castro R, Yarbuh I. Retention time and transport potential of eddies in the northwestern Gulf of Mexico. Ciencias Marinas. 2021;47(2):71–88. doi: 10.7773/cm.v47i2.3116.
82. Condie S, Condie R. Retention of plankton within ocean eddies. Global Ecology and Biogeography. 2016;25(10):1264-77. doi: https://doi.org/10.1111/geb.12485.
83. Allen CB, Kanda J, Laws EA. New production and photosynthetic rates within and outside a cyclonic mesoscale eddy in the North Pacific subtropical gyre. Deep Sea Research Part I: Oceanographic Research Papers. 1996;43(6):917-36. doi: https://doi.org/10.1016/0967-0637(96)00022-2.
84. Falkowski PG, Ziemann D, Kolber Z, Bienfang PK. Role of eddy pumping in enhancing primary production in the ocean. Nature. 1991;352(6330):55-8. doi: 10.1038/352055a0.
85. Dugdale RC. NUTRIENT LIMITATION IN THE SEA: DYNAMICS, IDENTIFICATION, AND SIGNIFICANCE1. Limnology and Oceanography. 1967;12(4):685-95. doi: https://doi.org/10.4319/lo.1967.12.4.0685.
86. GonzáLez-Ramírez J, Parés-Sierra A. Streamflow modeling of five major rivers that flow into the Gulf of Mexico using SWAT. Atmósfera. 2019;32(4):261-72.
87. Guerreiro CV, Baumann K-H, Brummer G-JA, Korte LF, Sá C, Stuut J-BW. Transatlantic gradients in calcifying phytoplankton (coccolithophore) fluxes. Progress in Oceanography. 2019;176:102140. doi: https://doi.org/10.1016/j.pocean.2019.102140.
88. Garcia-Romero F, Cortés MY, Lara-Lara JR, Rochín-Bañaga H, J. B, Aguirre-Bahena F, et al. Vertical fluxes of coccolithophores and foraminifera and their contributions to CaCO3 flux off the coast of Ensenada, Mexico. Ciencias Marinas. 2017;43:269-84. doi: 10.7773/cm.v43i4.2765.
89. Beaufort L, Lancelot Y, Camberlin P, Cayre O, Vincent E, Bassinot F, et al. Insolation cycles as a major control of equatorial Indian Ocean primary production. Science. 1997;278:1451-4.
90. Brown CW, Yoder JA. Coccolithophorid blooms in the global ocean. Journal of Geophysical Research. 1994;99(C4):7467-82.
91. Skampa E, Triantaphyllou MV, Dimiza MD, Gogou A, Malinverno E, Stavrakakis S, et al. Coccolithophore export in three deep-sea sites of the Aegean and Ionian Seas (Eastern Mediterranean): Biogeographical patterns and biogenic carbonate fluxes. Deep Sea Research Part II: Topical Studies in Oceanography. 2020;171:104690. doi: https://doi.org/10.1016/j.dsr2.2019.104690.
92. Hayat S, Skampa E, Gogou A, Stavrakakis S, Parinos C, Triantaphyllou M. Seasonal Variability in Present-Day Coccolithophore Fluxes in Deep Eastern Mediterranean Sea: A Multi-Year Study (2015–2017) of Coccolithophore Export in SE Ionian Sea at 4300 m Depth. Journal of Marine Science and Engineering. 2022;10(11):1761. PubMed PMID: doi:10.3390/jmse10111761.
93. Bonomo S, Placenti F, Zgozi S, Torri M, Quinci EM, Cuttitta A, et al. Relationship between coccolithophores and the physical and chemical oceanography of eastern Libyan coastal waters. Hydrobiologia. 2018;821(1):215-34. doi: 10.1007/s10750-017-3227-y.
94. Bonomo S, Schroeder K, Cascella A, Alberico I, Lirer F. Living coccolithophore communities in the central Mediterranean Sea (Summer 2016): Relations between ecology and oceanography. Marine Micropaleontology. 2021;165:101995. doi: https://doi.org/10.1016/j.marmicro.2021.101995.
95. Okada H, Honjo S. The distribution of oceanic coccolithophorids in the Pacific. Deep Sea Research and Oceanographic Abstracts. 1973;20:355-74.

96. Sprengel C, Baumann K-H, Neuer S. Seasonal and interannual variation of coccolithophore fluxes and species composition in sediment traps north of Gran Canaria (29°N 15°W). Marine Micropaleontology. 2000;39(1):157-78. doi: https://doi.org/10.1016/S0377-8398(00)00019-0.
97. Hamilton P, Lugo-Fernandez A. Observations of high speed deep currents in the northern Gulf of Mexico. Geophysical Research Letters. 2001;28(14):2867-70. doi: https://doi.org/10.1029/2001GL013039.
98. Kolodziejczyk N, Ochoa J, Candela J, Sheinbaum J. Deep Currents in the Bay of Campeche. Journal of Physical Oceanography. 2011;41(10):1902-20. doi: https://doi.org/10.1175/2011JPO4526.1.
99. Margalef R. Life-forms of phytoplankton as survival alternatives in an unstable environment. Oceanlogia. 1978;1(4):493-509.
100. Andruleit H, Stäger S, Rogalla U, Cepek P. Living coccolithophores in the northern Arabian Sea: ecological tolerances and environmental control. Marine Micropaleontology. 2003;49:157-81.
101. Linacre L, Lara-Lara R, Camacho-Ibar V, Herguera JC, Bazán-Guzmán C, Ferreira-Bartrina V. Distribution pattern of picoplankton carbon biomass linked to mesoscale dynamics in the southern gulf of Mexico during winter conditions. Deep Sea Research Part I: Oceanographic Research Papers. 2015;106:55-67. doi: https://doi.org/10.1016/j.dsr.2015.09.009.
102. Cushing DH. A difference in structure between ecosystems in strongly stratified waters and in those that are only weakly stratified. Journal of Plankton Research. 1989;11(1):1-13. doi: 10.1093/plankt/11.1.1.
103. Belkin N, Guy-Haim T, Rubin-Blum M, Lazar A, Sisma-Ventura G, Kiko R, et al. Influence of cyclonic and anticyclonic eddies on plankton in the southeastern Mediterranean Sea during late summertime. Ocean Sci. 2022;18(3):693-715. doi: 10.5194/os-18-693-2022.
104. Eppley RW, Rogers JN, McCarthy JJ. HALF-SATURATION CONSTANTS FOR UPTAKE OF NITRATE AND AMMONIUM BY MARINE PHYTOPLANKTON1. Limnology and Oceanography. 1969;14(6):912-20. doi: https://doi.org/10.4319/lo.1969.14.6.0912.
105. Behrenfeld MJ, Boss ES, Halsey KH. Phytoplankton community structuring and succession in a competition-neutral resource landscape. ISME Communications. 2021;1(1):12. doi: 10.1038/s43705-021-00011-5.
106. Jones HLJ, Leadbeater BSC, Green JC. Mixotrophy in haptophytes. In: Green C, Leadbeater BSC, editors. The Haptophyte Algae: Oxford University Press; 1994. p. 0.
107. Godrijan J, Drapeau D, Balch WM. Mixotrophic uptake of organic compounds by coccolithophores. Limnology and Oceanography. 2020;65(6):1410-21. doi: https://doi.org/10.1002/lno.11396.

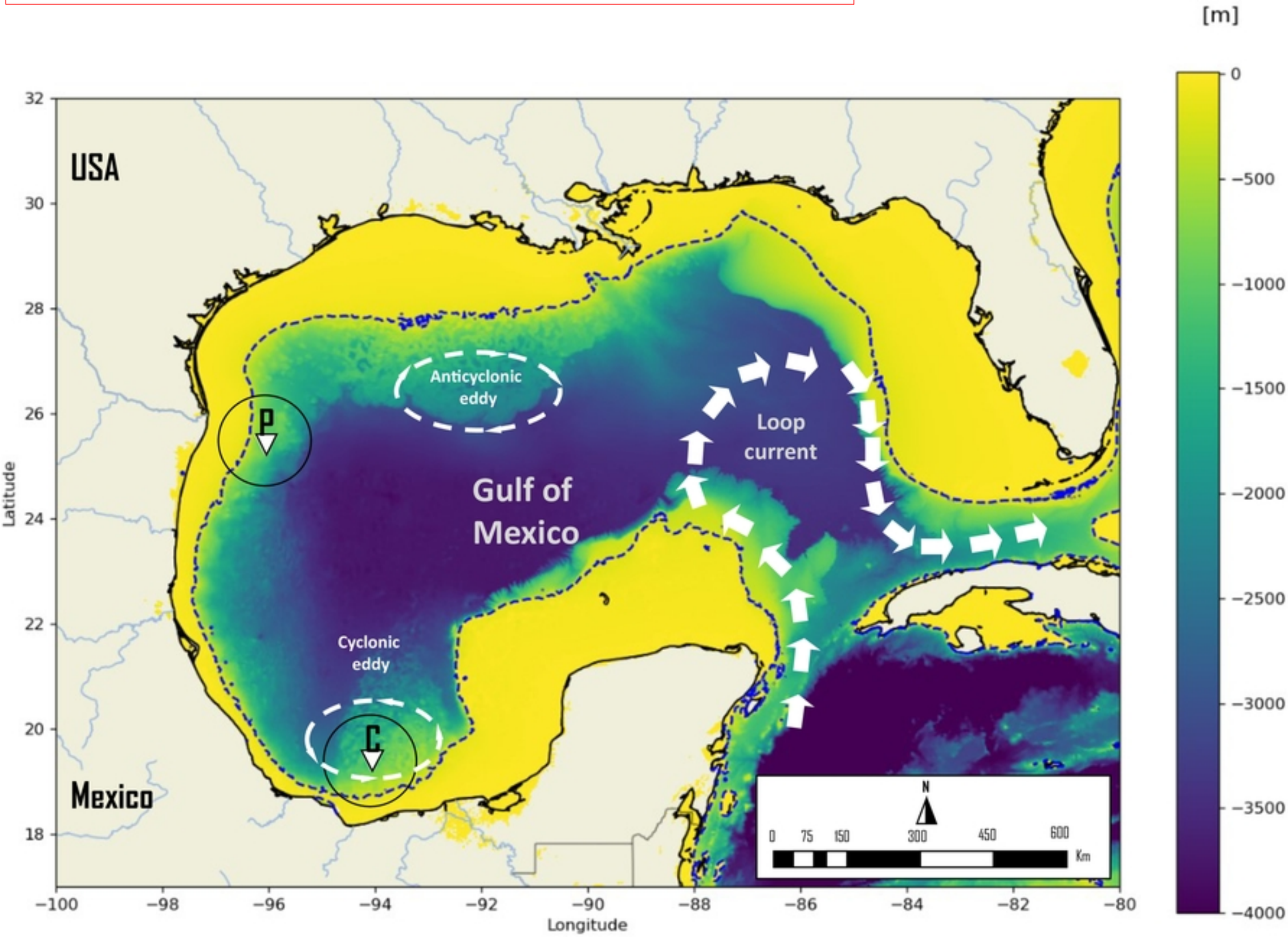
USA
Mexico
Gulf of
Mexico
Anticyclonic
eddy
Cyclonic
eddy
Loop
current
P
C
N
0 75 150 300 450 600
Km
Latitude
Longitude
[m]
0
−500
−1000
−1500
−2000
−2500
−3000
−3500
−4000
32
30
28
26
24
22
20
18
−100
−98
−96
−94
−92
−90
−88
−86
−84
−82
−80

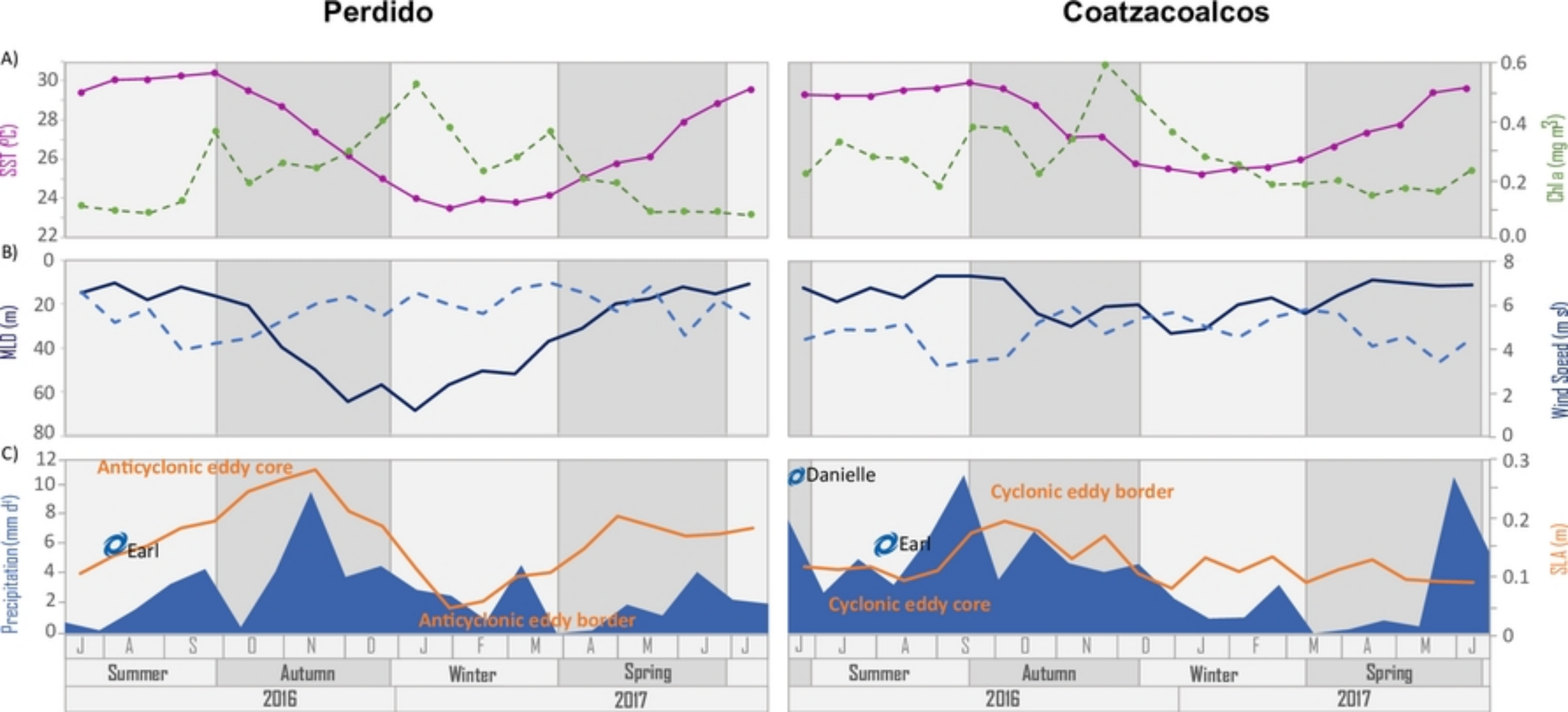
Perdido
Coatzacoalcos
A)
B)
C)
SST (°C)
Chl a (mg m^3)
MLD (m)
Wind Speed (m s^1)
Precipitation (mm d^1)
SLA (m)
Anticyclonic eddy core
Anticyclonic eddy border
Earl
Danielle
Cyclonic eddy border
Cyclonic eddy core
J A S O N D J F M A M J J
Summer
Autumn
Winter
Spring
2016
2017

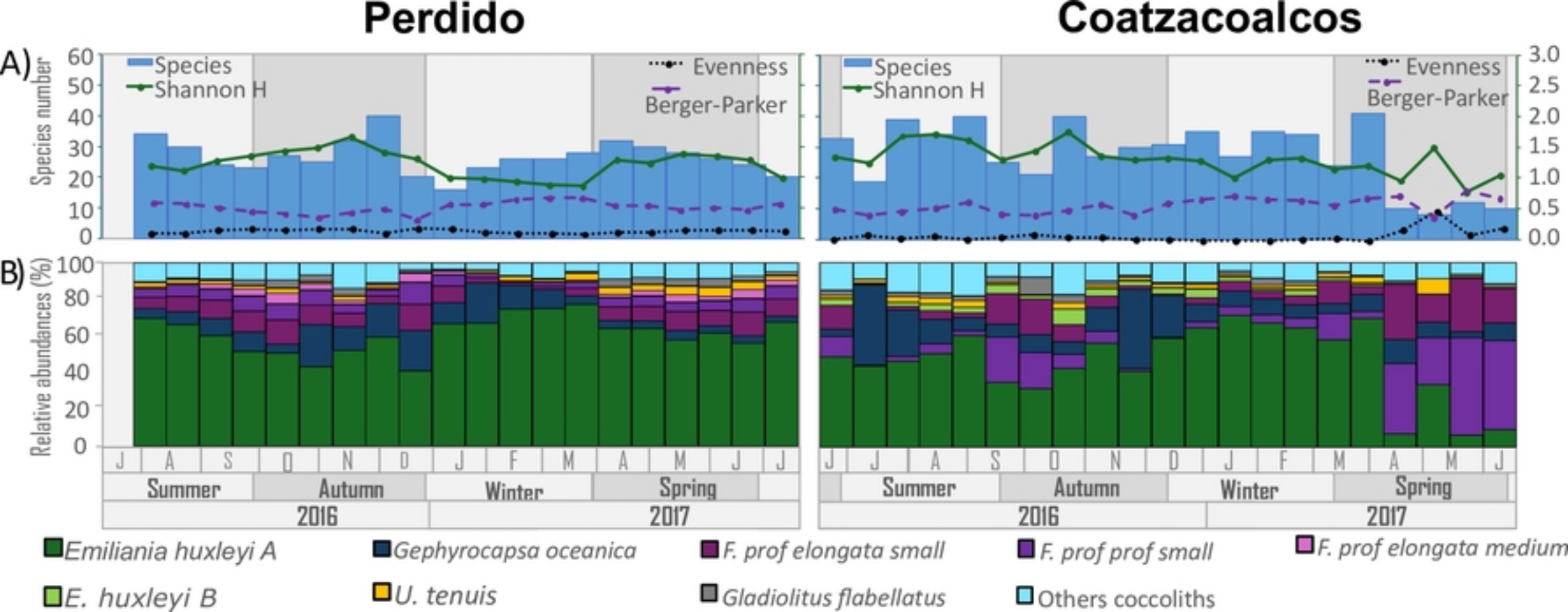
Perdido
Coatzacoalcos
A)
B)
Species number
Species
Shannon H
Evenness
Berger-Parker
Relative abundances (%)
J A S O N D J F M A M J J
Summer
Autumn
Winter
Spring
2016
2017
Emiliania huxleyi A
Gephyrocapsa oceanica
F. prof elongata small
F. prof prof small
F. prof elongata medium
E. huxleyi B
U. tenuis
Gladiolitus flabellatus
Others coccoliths

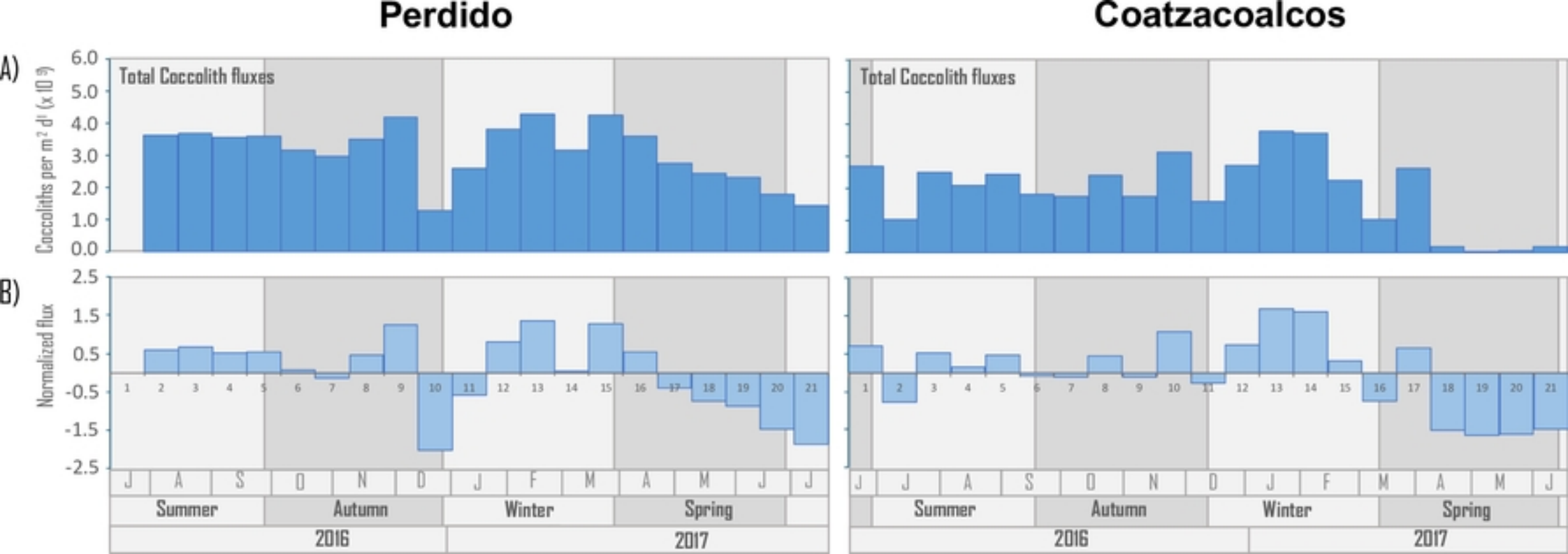
Perdido
Coatzacoalcos
A)
B)
Total Coccolith fluxes
Total Coccolith fluxes
Coccoliths per m² d¹ (x 10⁹)
Normalized flux
6.0
5.0
4.0
3.0
2.0
1.0
0.0
2.5
1.5
0.5
-0.5
-1.5
-2.5
1 2 3 4 5 6 7 8 9 10 11 12 13 14 15 16 17 18 19 20 21
J A S O N D J F M A M J J
J J A S O N D J F M A M J
Summer
Autumn
Winter
Spring
2016
2017

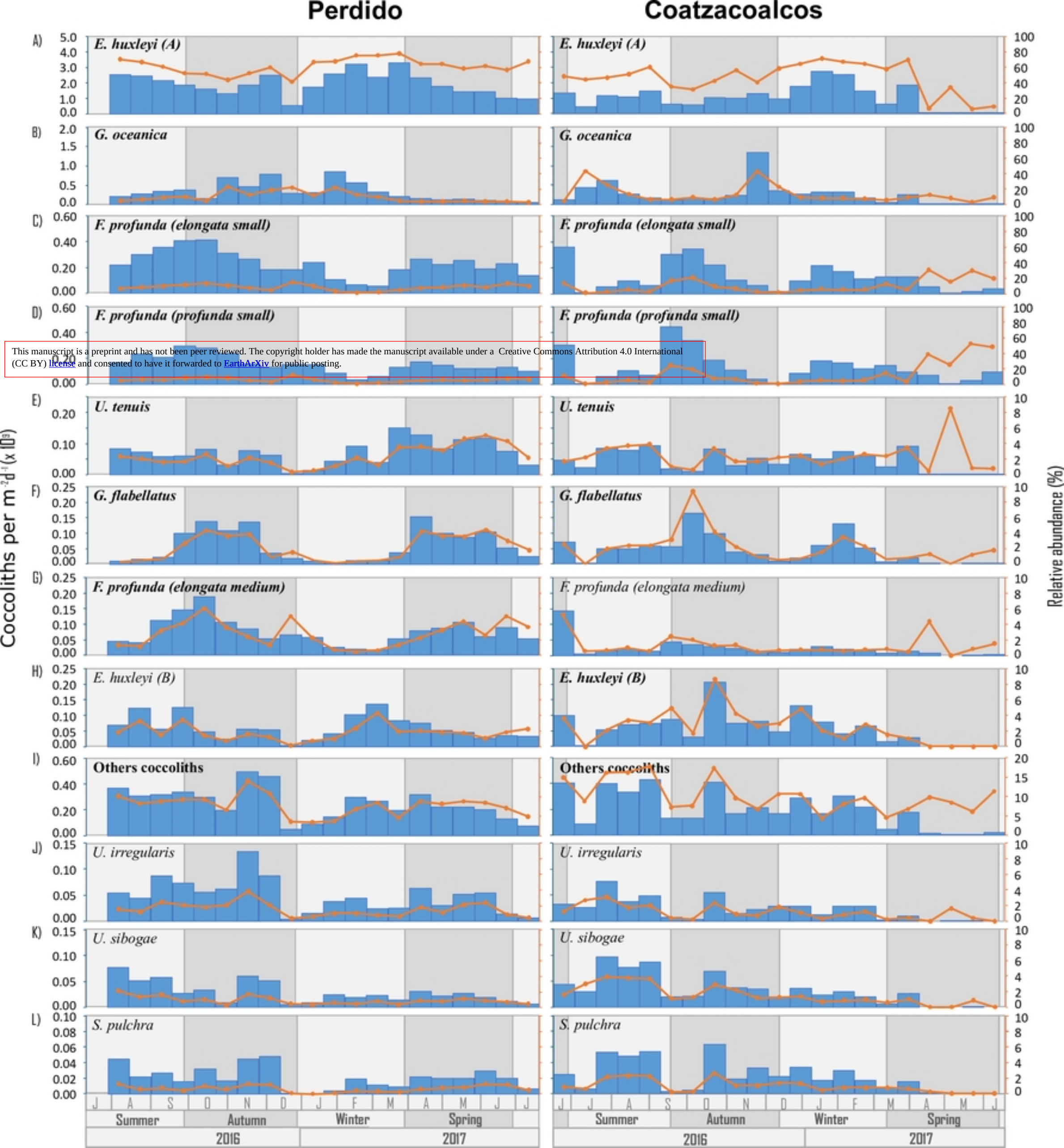

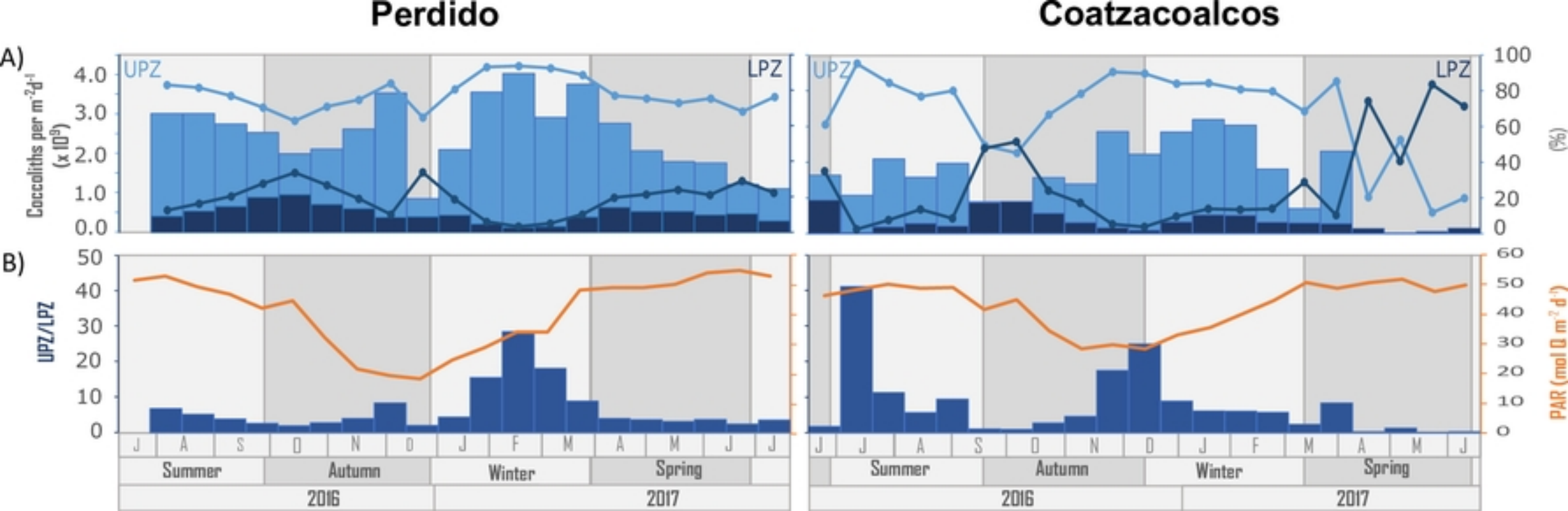
Perdido
Coatzacoalcos
A)
B)
UPZ
LPZ
Coccoliths per m-2d-1 (x 10^9)
(%)
UPZ/LPZ
PAR (mol Q m-2 d-1)
J A S O N D J F M A M J J
Summer
Autumn
Winter
Spring
2016
2017

A) Perdido

B) Coatzacoalcos

MLD
SLA
GOS
WND_S
PREC
PAR
SST
SSS
CHL
Total Flux
E. hux (A) ○
G. oce ○
F. prof (e s) ●
F. prof (p s) ●
U. ten ○
G. flab ●
F. prof (e m) ●
Other coccoliths
E. hux (B) ○
U. irr ○
U. sib ○
S. pul
F. prof (e l) ●
F. prof (p m) ●

1
0.333
-0.333
-1

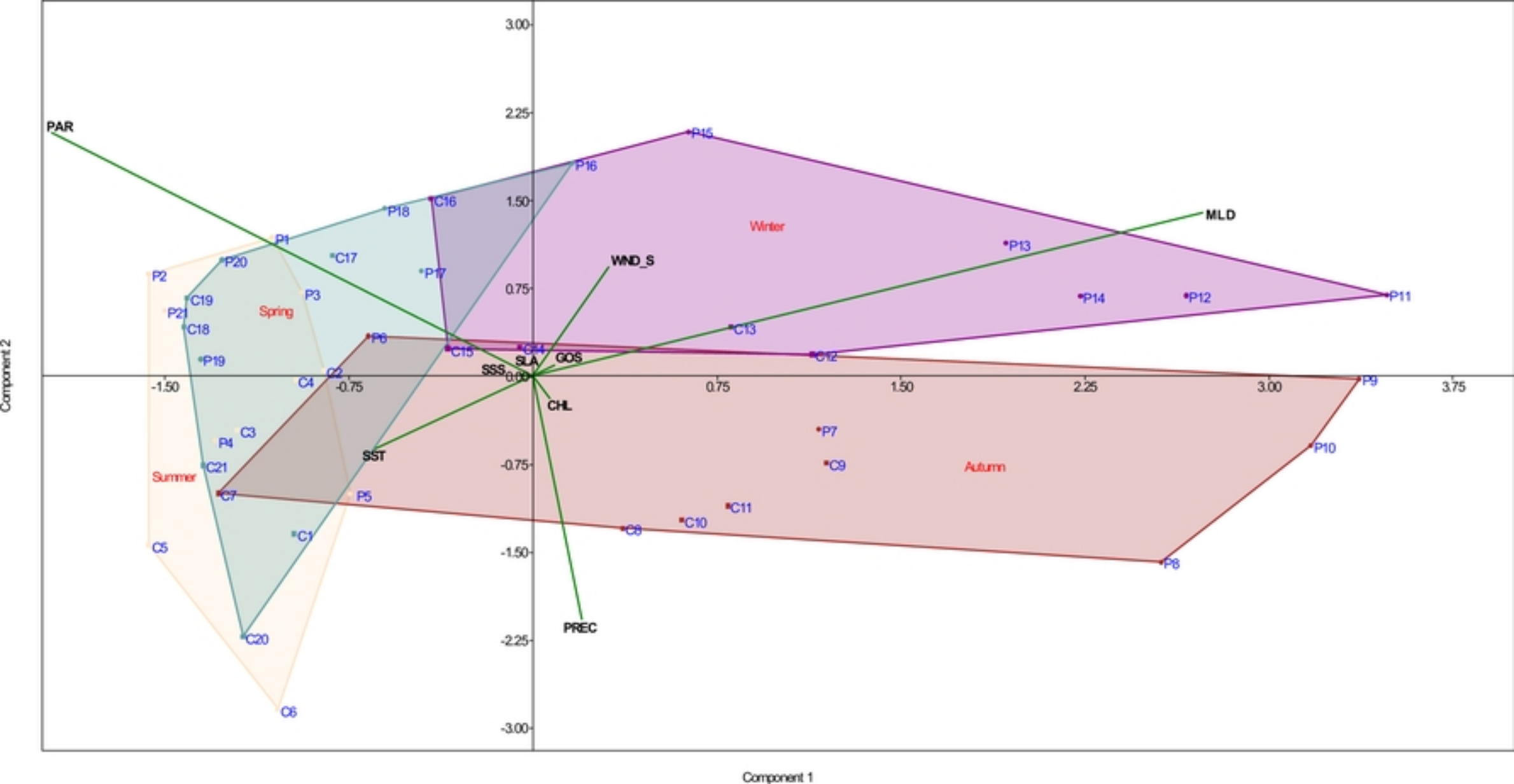
PAR
MLD
WND_S
PREC
SST
CHL
SLA
GOS
SSS
Winter
Spring
Summer
Autumn
P1
P2
P3
P4
P5
P6
P7
P8
P9
P10
P11
P12
P13
P14
P15
P16
P17
P18
P19
P20
P21
C1
C2
C3
C4
C5
C6
C7
C8
C9
C10
C11
C12
C13
C14
C15
C16
C17
C18
C19
C20
C21
3.00
2.25
1.50
0.75
0.00
-0.75
-1.50
-2.25
-3.00
-1.50
-0.75
0.75
1.50
2.25
3.00
3.75
Component 1
Component 2

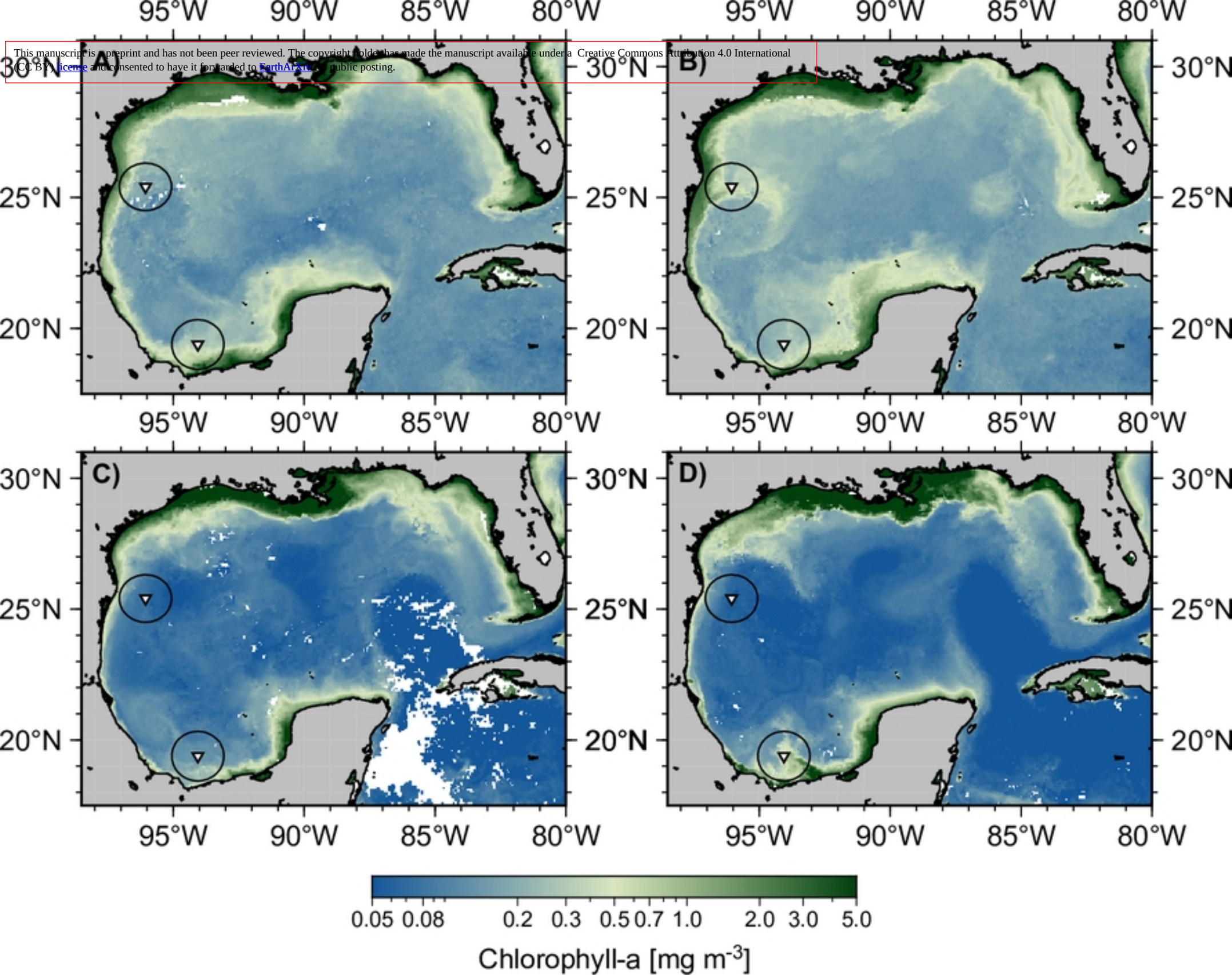

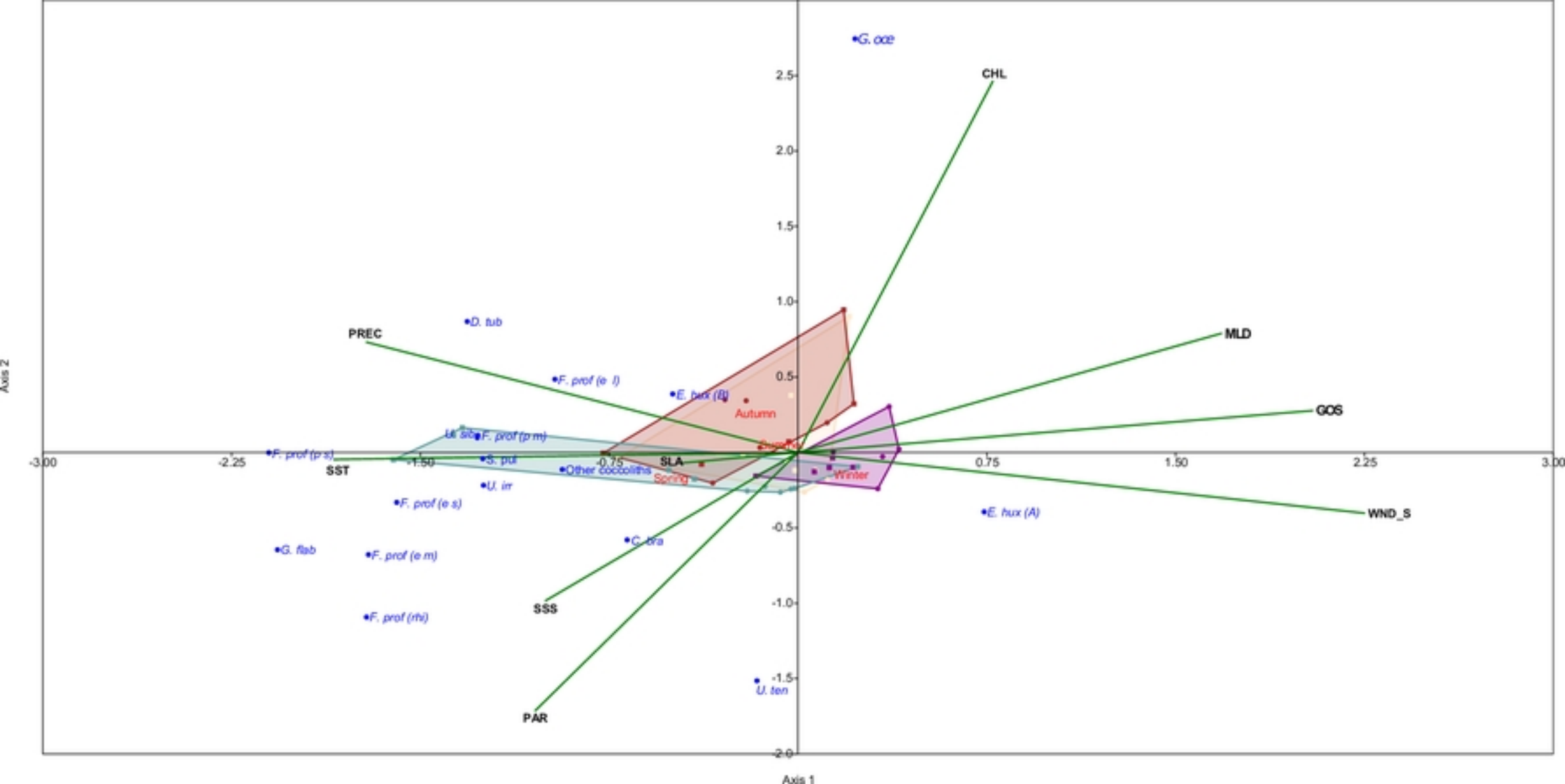
G. oce
CHL
D. tub
PREC
MLD
F. prof (e l)
E. hux (B)
Autumn
GOS
U. sic
F. prof (p m)
F. prof (p s)
S. pul
SST
SLA
Other coccoliths
Spring
Winter
U. irr
F. prof (e s)
E. hux (A)
WND_S
C. bra
G. flab
F. prof (e m)
SSS
F. prof (rhi)
U. ten
PAR
Axis 1
Axis 2
-3.00
-2.25
-1.50
-0.75
0.75
1.50
2.25
3.00
2.5
2.0
1.5
1.0
0.5
-0.5
-1.0
-1.5
-2.0